DESIGN, TESTING AND OPTIMIZATION OF A MICROFLUIDIC

DEVICE FOR CAPTURE AND CONCENTRATION OF BACTERIA

A Thesis

by

SRINIVAS CHERLA

Submitted to the Office of Graduate Studies of
Texas A&M University
in partial fulfillment of the requirements for the degree of

MASTER OF SCIENCE

August 2005

Major Subject: Mechanical Engineering

DESIGN, TESTING AND OPTIMIZATION OF A MICROFLUIDIC

DEVICE FOR CAPTURE AND CONCENTRATION OF BACTERIA

A Thesis

by

SRINIVAS CHERLA

Submitted to the Office of Graduate Studies of
Texas A&M University
in partial fulfillment of the requirements for the degree of

MASTER OF SCIENCE

Approved by:

Chair of Committee,   Ali Beskok
Committee Members,   N.K. Anand
                                  Suresh D. Pillai
Department Head,   Dennis O'Neal

August 2005

Major Subject: Mechanical Engineering

ABSTRACT

Design, Testing and Optimization of a Microfluidic Device for Capture and

Concentration of Bacteria.

(August 2005)

Srinivas Cherla, B. Tech., Jawaharlal Nehru Technological University

Chair of Advisor Committee: Dr. Ali Beskok

Effective detection of bacterial pathogens in large sample volumes is a challenging problem. Pre-concentration routines currently in practice before the actual detection process are cumbersome and hard to automate. An effort is made to address the problem of volume discrepancy between day-to-day samples and the concentrated samples needed for analysis. Principles of conceptual design are used in formulating the 'Need Statement', 'Function Structure' and in identifying the 'Critical Design Parameters' and 'Design Constraints'. Electrokinetic phenomena are used to exploit the surface charges on bacteria. Electrophoresis is used to transport the bacteria to electrode surface and "Electrostatic trapping" is then used to capture these microbes on the electrode surface. The captured microbes can then be concentrated in a concentrator unit.

A prototype microfluidic device is fabricated for showing the proof of concept. Optimization is done to minimize hydraulic power consumption and wetted volume. Observations from the initial prototype device along with the optimization results are used in building a new prototype device. Operation of this device is demonstrated by capture of bacteria from flow. Qualitative studies are conducted and preliminary quantification is also done.

To my Parents

ACKNOWLEDGEMENTS

TABLE OF CONTENTS

LIST OF TABLES

LIST OF FIGURES

CHAPTER I

INTRODUCTION AND LITERATURE REVIEW

1.1 WATER QUALITY AND MONITORING

Detection of bacterial pathogens has always been a challenging task. Since the invention of microscope and the first documentation of micro-organisms by Anton van Leeuwenhoek circa 1680, microbiologists have come a long way in the technologies for identifying bacterial pathogens. Though we have a better understanding of microbes and their role in causing disease, we still have a lot to learn in this field. It is estimated by WHO/UNICEF that two out of every five people in the world lack improved water sanitation and that accounts to nearly 6000 deaths per day [1]. Studies by Mroz et al. revealed the presence of fecal coliforms and bacterial pathogens in domestic wells that normally go undetected in standard methods of water testing [2]. This calls for an immediate effort to develop a universal water quality monitoring system. A good water quality monitoring system has to be unsophisticated, automated, and rapid in detection and identification of pathogens. It has been found out that molecular-based approaches show the greatest promise for the development of a unified system for multiple waterborne pathogen detection [3,4]. Some of the established technologies in this direction are NMR (Nuclear Magnetic Resonance) and PCR assays (Polymerase Chain Reaction). However, these devices need small and concentrated test samples to deliver

_____

This thesis follows the style of journal of *Numerical Heat Transfer.*

accurate results. But, drinking water samples generally have large volume and they do not have bacterial pathogen concentration that can be detected by such devices. For instance, if the water authorities have to maintain optimal sanitary conditions in water catchments and distribution systems, they must have easy access to rapid and accurate water quality data, including an indication of bacteriological quality. Water-testing laboratories commonly evaluate bacteriological water quality by using methods that assess the number of bacteria in water samples that are able to form visible colonies in a growth medium, under specified test conditions (e.g. medium nutrients, incubation time, incubation temperature, etc.). In addition to taking a long time (as long as a couple of days), these techniques can only be used to quantify the presence of culturable heterotrophic bacteria [5]. The problems mentioned above need to be effectively solved in unified water quality monitoring systems, to ensure that the water quality is fit for consumption.

1.2 WATER BORNE PATHOGENS – DETECTION ISSUES

Bacteria are notorious for their universal presence even in the most hostile environments. In spite of their ubiquitous presence, bacteria have been found to preferentially settle down on surface of solids (e.g. rocks in water streams) or at the interface between water and air as shown by the studies of Van Loosdrecht et al. [6]. Powell et al. [7] have studied and quantified the deposition and removal of bacterial cells onto glass surfaces. They found that interfacial tension between fluid and the collector surface has profound effect on the initial deposition rate of bacteria onto surfaces. Rutter et al. [8, 9] suggested that the time a bacterial cell spends in the vicinity of the surface helps it build polymer bridges that are seen as the primary attachment mechanism.

Pathogenic strains of bacteria in particular, operate by the mechanism of transport, initial adhesion, attachment and colonization. This suggests that the bacteria are not uniformly distributed in any medium and might be concentrated in some areas while scarce or not present in other areas. With the current state of the art detection systems, one can detect microbes only if their concentration is above a certain level. Also the accuracy of these results depend on the location from where the sample is collected and whether it has a high enough concentration of bacteria. This brings up the problem of bacterial detection when they are present in very low concentrations.

There are some other issues associated with easy detection of bacteria. Microorganisms in the environment are exposed to hostile conditions that threaten their survival. Aertsen et al. [10] in their review, mention that bacteria undergo a process of self-inactivation in order to cope up with constantly changing stress conditions, governed by the surrounding environmental factors. Such bacteria are often defined as 'Viable but nonculturable' (VBNC). It means that the bacteria exhibit measurable traits of physiological activity but fail to grow to a detectable level [11]. For example, chlorine used for disinfecting potable water may cause sub lethal injury of some bacteria, thereby rendering them non-culturable [12, 13]. They may however revert back to a state of culturability under a different set of environmental conditions [14]. This limits the usage of culture-based methods in estimating the bacteriological quality of water or even the simple detection of bacteria.

From the discussion above, it can be seen that there is a need for technology that can reliably assess the bacteriological quality of water. Significant amount of research has been done in trying to overcome the above-mentioned problems. Benoit et al. [15]

summarize all currently available methods for rapid separation and concentration of bacteria in food samples. These can broadly be divided into physical methods (such as filtration [16] and centrifugation [17]) and adsorption methods (such as immunomagnetic separation [18] and dielectrophoresis [19]). Each method has its own advantages and disadvantages. Molecular based methods like PCR assays are the most reliable among currently available technologies [3]. However the general test sample volume for most of the PCR based assays is on the order of microliters to milliliters and has to be a concentrated sample. In other words, a dilute sample having a volume of one liter will have to be concentrated 1000 fold to result in a sample volume that can be used with a PCR assay. So there is need for a device that can concentrate microbes from large volumes down to a sample volume that can be used with well-established detection techniques like PCR assays.

Recent advances in the field of biotechnology and bioengineering have enabled research and study into the nature of microbial interaction with surfaces of solids. It has been observed that surface characteristics of both bacteria and the substrate materials have a profound influence on bacterial adhesion and growth process. Relatively hydrophobic and highly negatively charged strains migrated faster than hydrophilic and less negatively charged strains. Burchard et al. [20] observed that gliding was inhibited on the very hydrophobic substrata and skittish on the very hydrophilic substrata. Different microorganisms also exhibit different types of behavior when interacting with surfaces. *Escherichia coli (E. coli)* exhibits ''near-surface swimming'' behavior and migrates over surfaces [21], which was explained by Vigeant and Ford as a form of reversible adhesion with residence times of over 2 minutes [22]. Studies by Poortinga et

al. [23] showed that some bacteria have different cell structure with long surface appendages and show deviation from usual behavior on near surface adhesion. In addition, there are issues with biocompatibility of substrate materials and toxicity to humans on prolonged use. All the above factors have to be carefully considered in developing the unified water quality detection system.

1.3 MICRO-FLUIDICS

Ever since Nobel Laureate Prof. Richard P. Feynman's famous quotation "There's Plenty of Room at the Bottom" on December 29th, 1959, the study of micro/nano systems has seen a surge and has attracted a lot of research interest [24]. Since their inception in the 1970's, micro/nano technology became widely accepted in the 1990's after some commercial success, and started being widely referred to as MEMS (Micro Electro Mechanical Systems) [25, 26]. Microfluidics is a branch of MEMS that deals with the study of motion of fluids at micro-scale. The ultimate goal of Microfluidics is to understand the principles of fluid flow at micro scales, and apply that understanding in developing devices that can replace large fluid handling systems. However the principles applied to macro scale systems cannot directly be applied to micro scale systems. Karniadakis and Beskok discuss many aspects and challenges in detail [27]. Microfluidic systems comprising nozzles, pumps, reservoirs, mixers, valves, etc., can be used for a variety of applications including drug dispensing, ink-jet printing and general transport and mixing of liquids and gases. Advantages of microfluidics compared to conventional fluidic systems are: low fabrication cost, mass manufacturing ability, short time scales for analysis, low power requirements, enhancement of analytical performance, and low consumption of chemicals and other reagents [28].

Knowing all these benefits, it makes sense to explore the usage of these microfluidic devices for applications where conventional devices have been the accepted norm. As discussed above, the analysis of water quality in water distribution systems is one such area. As an interdisciplinary research project, our group is trying to address this problem by developing a microfluidic device that can take large volumes of water as input and deliver small test samples to bacterial detection systems like PCR assays. One can exploit the surface characteristics of bacteria and viruses and use microfluidic phenomenon to collect the bacteria, which can then be used to prepare a concentrated test sample for the purpose of detection. This will considerably reduce the sample preparation routines, before being tested using currently available bacterial detection systems.

1.4 ORGANIZATION OF THE THESIS

The organization of this thesis is as follows. In Chapter II the need for development of the proposed microfluidic capture and concentration device is analyzed using design methodologies. A function structure is generated, design parameters and constraints are identified. Chapter III outlines the design concept for the device and principles that govern its operation. Chapter IV describes the experimental setup, fabrication and testing of the device. The results of experiments and related discussion of qualitative and quantitative studies are presented in Chapter V. Conclusions and recommendations for future work are included in Chapter VI.

CHAPTER II

PHASE I: NEED ANALYSIS AND FUNCTION STRUCTURE

2.1 NEEDS AND OBJECTIVE OF THE PROJECT

In December 1999, NASA outlined its 'Advanced Environmental Monitoring and Control Project Plan' (AEMC). It deals with understanding the internal environment of a space ship and analyzing its composition, followed by development of related monitoring technologies. One of the projects goals was to 'Obtain state of the art, revolutionary technologies for spacecraft environmental monitoring and control' [29]. From the background and literature survey, it can be seen that there is lack of a robust water quality monitoring system in the water distribution system of the spacecraft. There is a need "To design a device that addresses the problem of volume disparity between distribution systems and microbial detection systems, is autonomous and maintenance free, is quick and highly efficient, is compact and economical in power requirements and has a service life longer than the interplanetary space missions." The objective for this project is to develop and demonstrate the working of a device that takes large volumes of water as input, concentrates pathogens in it and delivers a tiny sample with a volume that is compatible with current bacterial detection systems.

2.2 DESIGN METHODOLOGY

The guidelines on design methodologies developed by the Institute for Innovation and Design in Engineering (IIDE) at Texas A&M University are followed and our knowledge on the behavior of bacteria is used, to deliver a device that achieves

the stated objective. IIDE design methodologies assist the design process by easily identifying, "What needs to be done" and helping the designer to come up with innovative solutions to a "Need" [30, 31]. The entire project is thereby divided into four different phases as follows:

Phase I (Need Analysis and Function Structure)

Phase II (Conceptual Design)

Phase III (Design Embodiment and Product Creation)

Phase IV (Demonstration of Quality)

In the first phase, the given problem is defined in a technically precise, yet abstract manner so as to provide a correct direction to the design process. The definition should be unambiguous and at the same time it should be abstract enough so as not to automatically lead to a solution. The motive of need analysis is to identify the need and
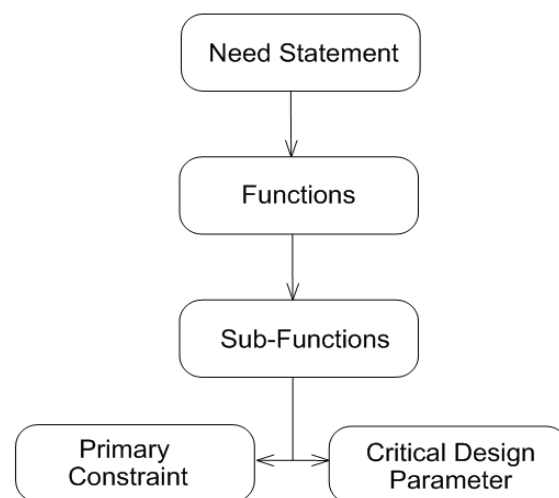
FIGURE 2.1: Function structure hierarchy.

 try to determine all the functions that are to be performed by the device, while simultaneously satisfying the design specifications and constraints.

Once the need is identified, an iterative process called abstraction is used to generate a need statement. Abstraction is the process of progressively transforming a general design task into a functionally precise definition of need in technically fundamental terms. A need statement is followed by function structure, which is the representation of all functions and sub-functions that need to be performed by the design while satisfying all the constraints. It also helps us identify the 'critical design parameters' and 'primary constraints' for each function. The critical design parameters are later on quantified in design process. Figure 2.1 illustrates how a need statement leads to identification of primary functions and critical design parameters.

Having identified the need in first phase, we move to the second phase of design where we generate design concepts based on some governing laws and physical principles that can solve our problem. Each concept has to meet the functional requirements and satisfy all the constraints. These concepts are then evaluated based on criteria like economy; ease of manufacture etc., and the concept that fares best among
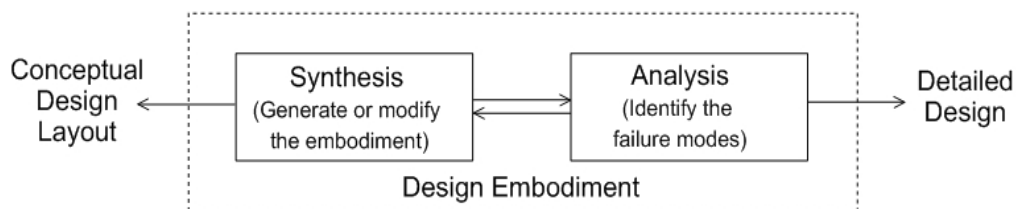
FIGURE 2.2: Design embodiment.
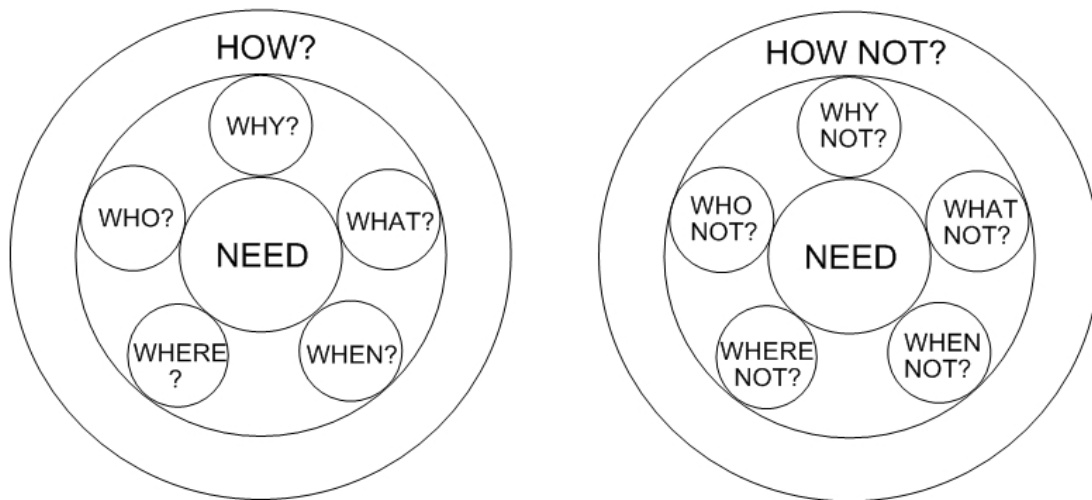
FIGURE 2.3: Need abstraction.

them is pursued for design embodiment and further design realization. In the next phase (Phase-III), we iteratively synthesize and analyze the conceptual design to get a final design layout.

During synthesis, the conceptual design layout is embodied and a detailed physical representation of design is created. This embodiment is then analyzed to check for any pitfalls and the feedback is used in further synthesizing the design embodiment. This process iterates till a satisfactory solution emerges where all the possible failures have been accounted for. Figure 2.2 illustrates the design embodiment process. It is followed by engineering drafting, assembly and test procedures that are to be used in the manufacture and assembly of product. The final phase (Phase-IV) involves actual production of a prototype device for demonstrating its working quality and functionality. The flaws revealed during testing of this prototype device are then corrected by modifying the design accordingly.

2.3 NEED STATEMENT AND FUNCTION STRUCTURE

Need Abstraction is done by answering the basic questions of 'How?' and 'How Not' about the "Need". This leads to answers that reveal the true need statement, as better illustrated in Figure 2.3.

On going through the need abstraction process, the need statement is defined as follows: "To design a device that addresses the problem of volume disparity between distribution systems and microbial detection systems, is autonomous and maintenance free, is quick and highly efficient, is compact and economical in power requirements and has a service life longer than the interplanetary space missions." Once the seed statement is defined, the function structure is generated based on it. Primary design
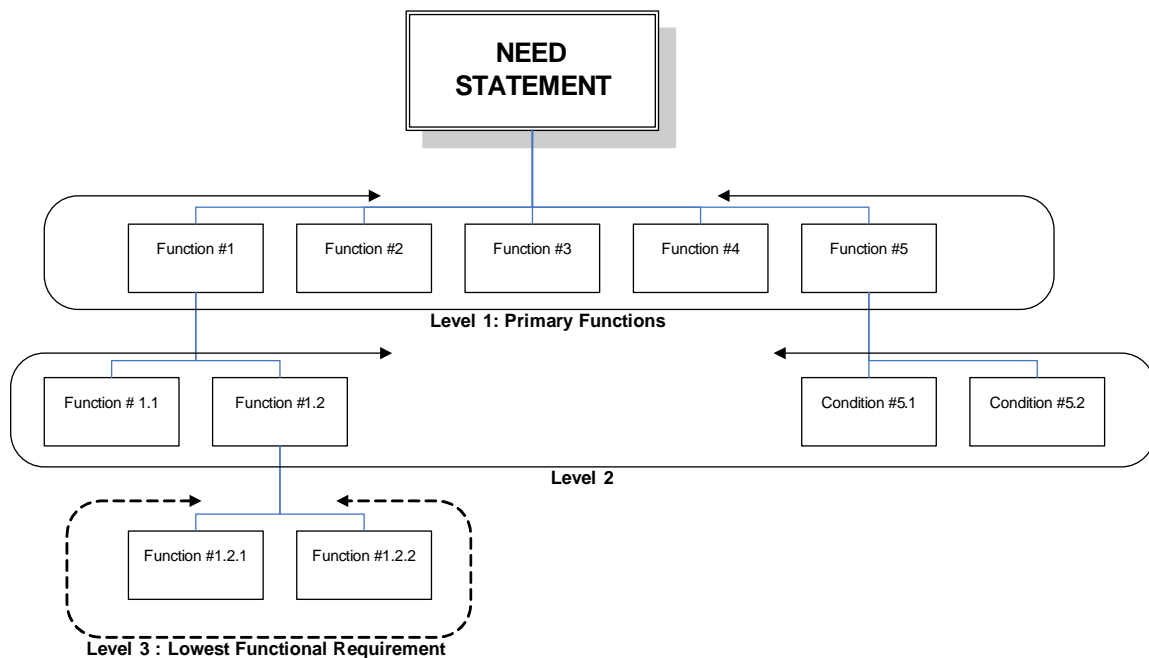
FIGURE 2.4: Generic function structure.

functions are first identified. These primary functions are further broken down into sub-functions or lower level functional requirements. By satisfying each of these sub-functions, which have in turn been derived from the main need statement, one can effectively develop a design that satisfies the need. Associated with each sub level functional requirement are a critical design parameter and a design constraint. A design parameter is a scientific variable that governs the functional requirement. It is chosen so that it can be easily quantified. The design constraint sets a range limit on the design parameter or specifies a condition under which the functional requirement has to be satisfied. Figure 2.4 shows a generic function structure with the primary functions and sub functions of those primary functions.

2.4 DESIGN PARAMETERS AND CONSTRAINTS

From the need statement, it is seen that the primary functions for the device are capture of a variety of pathogens, isolation from main flow and concentration of the separated bacteria. The device should also be reliable and robust. For concentrating the bacteria, we first have to capture them, thus we in turn introduce another primary function, i.e. capture. Apart from the primary functions, the device has to be extremely reliable in its operation. So we also include this property in the primary requirements. To perform the primary functions, the device might have to perform a couple of other simple sub-functions. These sub-functions form the next level of the function structure. This process is continued till one reaches a fundamental quantifiable parameter, which is called the "Critical Design Parameter" for that sub-function. The function structure for capture and concentration device is shown in the Figure 2.5. In the Figure 2.5, 'C' stands for design constraint and 'P' stands for critical design parameter. Knowing the design

To design a device that addresses the problem of volume disparity between distribution systems and microbial detection systems, is autonomous and maintenance free, is quick and highly efficient, is compact and economical in power requirements and has a service life longer than the interplanetary space missions
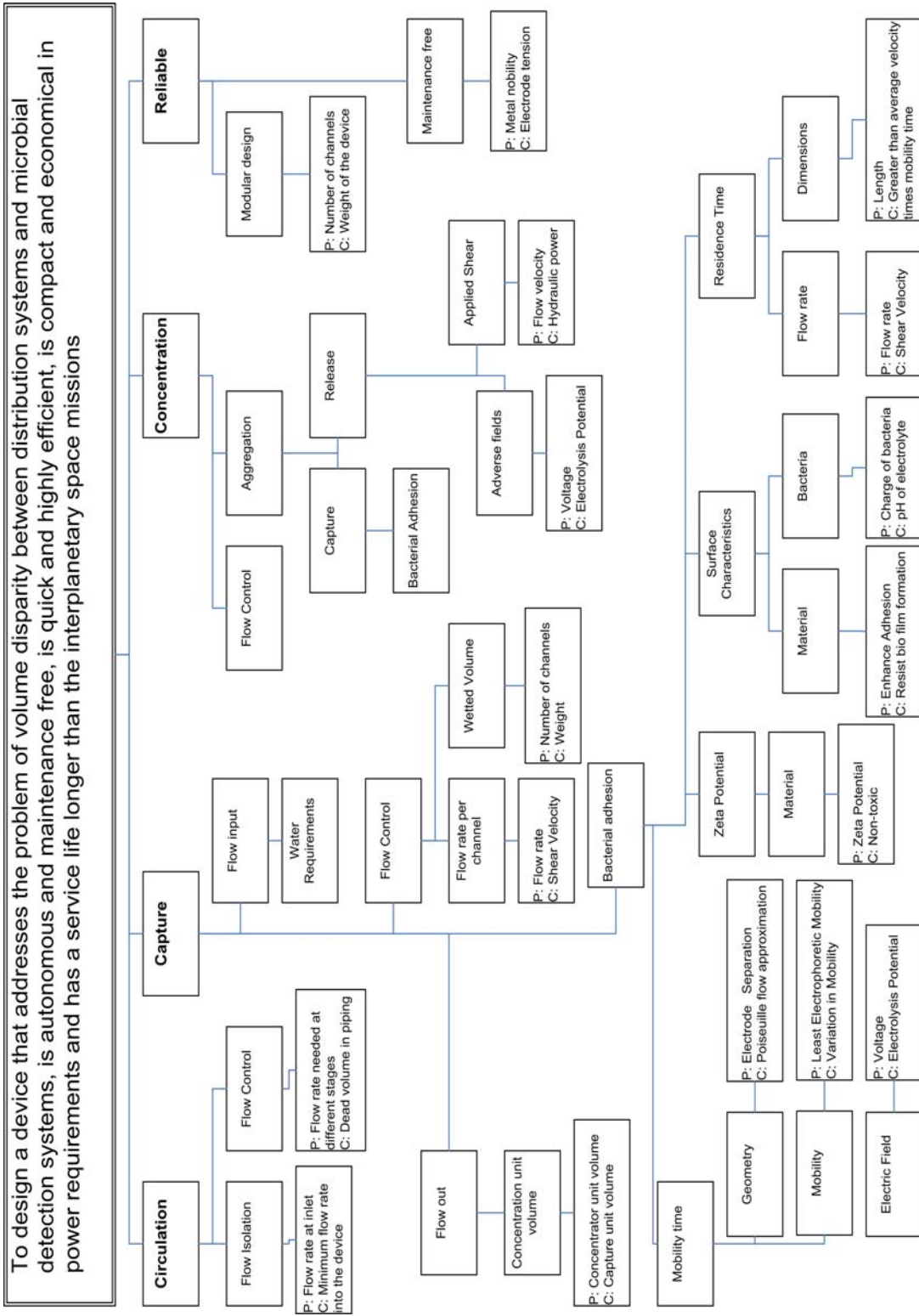
FIGURE 2.5: Function structure for a capture and concentration device.

 parameters and their respective constraints, procedures to quantify these parameters are identified. The design parameters in our function structure are:

Flow Rate: The device has to be designed for a certain range of flow rates. Designing the device for a maximum flow rate will ensure that it functions below that flow rate. The maximum flow rate should be given for design. Also since the device is an inline component, the volume flow rate in the water distribution system should be known so as to isolate only the volume that can be processed by the device. Further, the device dimensions and the total number of modules will also be decided by the flow volume to be processed.

Number of Channels: Number of channels decides the wetted volume of the device. Since weight of the device and its volume are directly proportional, minimizing the volume takes care of the device weight. The maximum weight the device can have sets an upper limit on the volume of the device.

Electrode Separation: Electrode separation is one factor that determines the migration time for bacteria. Smaller the electrode separation, lower the migration time and higher the hydraulic power requirements. The ratio between channel separation and the width of electrode must be high to satisfy Poiseuille flow approximation that is used to characterize flow in the channel.

Electrophoretic mobility: It is a parameter that tells us about the speed of motion of bacteria purely under the influence of an electric field. For high efficiency in the capture of bacteria, it is necessary that even the bacteria with lowest mobility be captured before the fluid leaves the channel. This means that the mobility time for the bacteria should be less than the residence time.

Voltage: Voltage applied across the device affects the speed of capture and strength of bacterial adhesion. The maximum voltage that can be applied is limited by the electrolysis potential for water (1.23V). So an optimum voltage is to be applied for capture to occur, while avoiding any electrochemistry with water.

Zeta potential: Zeta potential is the electrokinetic potential at the end of the Stern-layer in an Electric Double layer [28]. The current device works just on electrophoresis, so the zeta potential of channel walls has to be zero to avoid electroosmosis, which is undesirable in this case.

Charge of bacteria: It is important that bacteria maintain their charge during the process of capture and concentration. Any change in the amount of charge can render the device useless. pH of water significantly affects the charge of bacteria, and so it should remain constant for proper working of the device.

Device length: Residence time of bacteria is solely dependent on the length of channel. We must choose an appropriate length such that the residence time of bacteria is greater than their mobility time to ensure full capture.

Flow Velocity: Once the bacteria are captured, they have to be concentrated. This is done by flushing the fluid at high velocity to shear off all the captured bacteria.

Metal nobility: Electrode material should be noble. It should not get involved in any sort of electrochemistry. Metals like Gold and Platinum are possible choices. It should also be non-toxic, since water from the device will directly be supplied into water delivery system. Similarly the process should not yield any byproducts that will make it unfit for consumption. For example substantially modify the mineral contents in water, change its pH or lead to toxic products.

The next phase in the design process is to generate a design concept based upon the function structure. The function structure also helps us find the critical design parameters and design constraints that help in the design process. The concept generated is then given a physical embodiment resulting in a prototype device. This prototype device is tested and the results obtained are used to further optimize the device design.

CHAPTER III

PHASE II: CONCEPT GENERATION FROM THE NEED

3.1   EVOLUTION OF CONCEPT

Once the need analysis is done and a function structure generated, a design concept that is able to address the "Need" is produced. This design concept should be based on some fundamental scientific principles, governing laws or constitutive relations that can be exploited to address the need. The principles of conceptual design outlined by IIDE, help in coming up with innovative ideas and creating effective embodiments in the design process. This conceptual design is then tested to see if it meets all the design requirements. If the concept survives this test, it is a viable design and is considered for further design embodiment. This chapter deals with concept generation from the need statement and function structure.

From the function structure, it can be seen that bacteria have a charge on them. This suggests that it is possible to use electrostatic attraction to capture the bacteria from a large volume. These captured bacteria can then be concentrated into a smaller volume by suitable concentration mechanism. The underlying hypothesis in operation of the device can be stated as: "Electrophoretic transport followed by Electrostatic trapping" can be employed in a microfluidic device to capture and concentrate microorganisms from large volumes of water. The device will basically work in two steps, the capture stage and the concentration stage.

Capture – It is hypothesized that the negative charges on microorganisms can be exploited to trap them using positively charged electrodes.

Concentration – The capture phase is followed by a concentration phase where the captured contents are passed into another similar device where concentration will be achieved. Modular design of these devices and difference in their volumes will enable simultaneous capture and concentration.

It is further hypothesized that once the microbial contaminants are captured and concentrated using the microfluidic device, the concentrated sample generated will be suitable for analysis in any of the existing or future pathogen detection technologies.

3.2   DESCRIPTION OF CONCEPT

A simple functional line diagram of the proposed device is shown in Figure 3.1. Main components of design are the two capture units having the same wetted volume, and a concentrator unit that has a wetted volume compatible with microbial detection and analysis systems. The large volume difference between the capture and concentration units proves to be a challenge in integrating microfluidic devices (e.g. concentrator) with macroscopic applications (in regards to the volume compatibility and time scales).

This problem is addressed by employing an additional capture unit (capture unit II), which has a volume identical to the capture unit I. Capture cycle is run continuously for an hour to ensure efficient particle collection from the high volume input flow *(for our case it is 5 L/hr)*. Thus microbial contaminants that are in the water distribution line
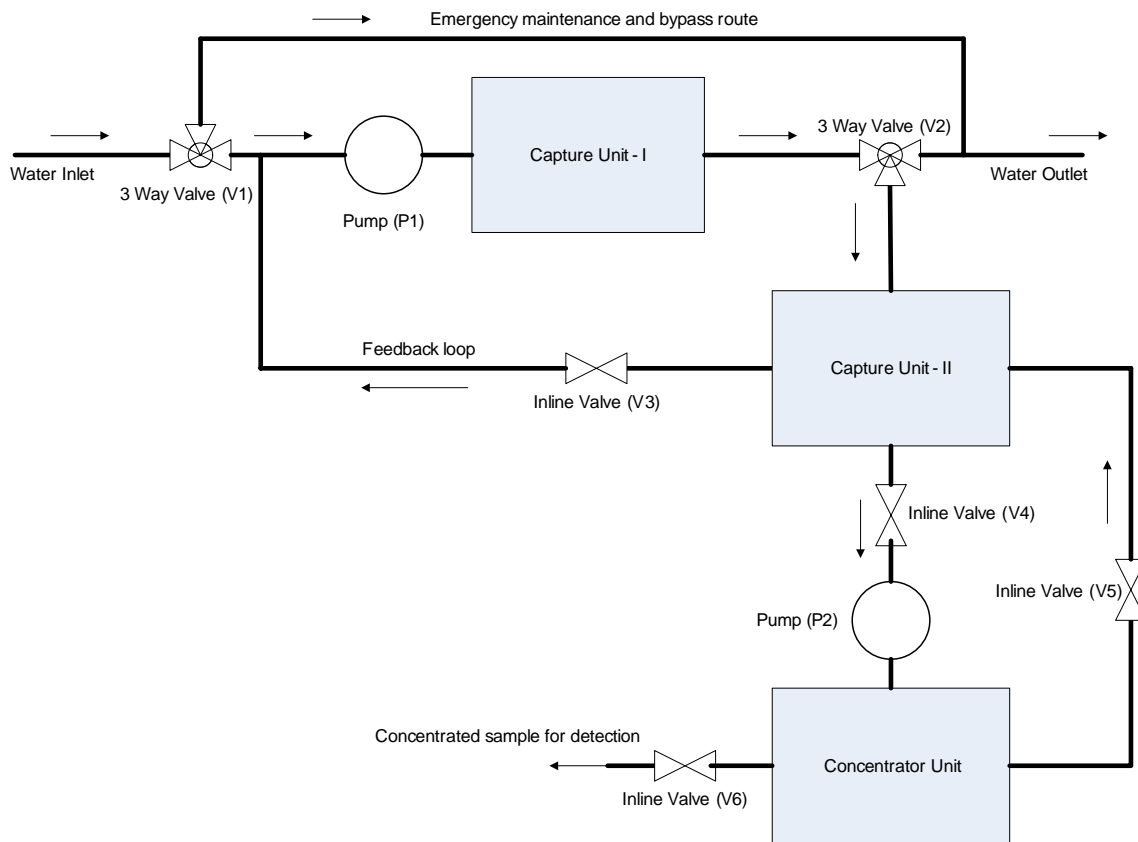
FIGURE 3.1: Functional diagram of a water quality monitoring system.

are captured in capture unit I. Once the capture step is completed, microbial contaminants will be flushed to the capture unit II. This step should take only a couple of minutes since both the capture units have same volume. After this quick-flush, capture unit I will return to its basic capture process, while the contents of capture unit II will be pumped through a sample concentration unit to reduce the sample volume (equal to capture unit II wetted volume) to 1mL. This output volume can be accommodated by most of the current microbial detection systems. After the capture and concentration stages, the samples are sent for detection.

TABLE 3.1: Water flow routine for the capture and concentration unit

Operation	Valves						Pumps	
	V1	V2	V3	V4	V5	V6	P1	P2
Capture	To Cap #1	To Outlet	Closed				On	
Quick Flush	To bypass	To Cap # 2	Open	Closed	Closed		On	
Concentration		To Outlet	Closed	Open	Open	Closed		On

In the current design, capture and concentration operations continue simultaneously. In addition to allowing simultaneous capture and concentration operations, one of these capture units can also double up and take the function of both the units in an event where one of the units fails. Typical operation cycle of the device shown in Figure 3.1 is represented in tabular form here.

In Figure 3.1 and Table 3.1, 'P' and 'V' identify pumps and valves respectively. V1 and V2 are two-way valves, and they switch between the two outlets indicated, while V3-V6 are inline valves. Emergency shutdown and maintenance bypass system is also included (V1). Pump P1 maintains desired flow in the particle capture system. Once recycled water is passed through the particle capture system, it is dispensed for use.

3.3 EXPLANATION OF GOVERNING PRINCIPLES

Electrokinetic phenomenon, in particular, electroosmosis and electrophoresis govern the device functioning. Electrokinetic phenomena arise due to formation of 'Electrical Double Layer' (EDL) at the interface between a dielectric wall surface and an ionic solution. Reuss [32] first observed electrokinetic phenomena in 1809, while investigating the effect of electric field on porous clay. Helmholtz developed the electric
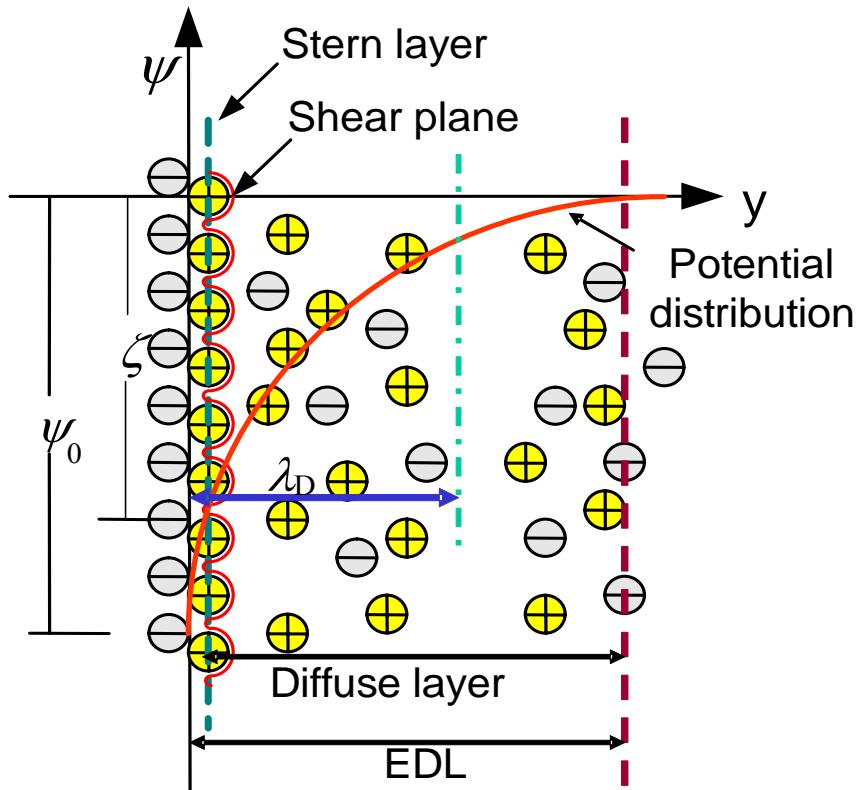
FIGURE 3.2: Schematic diagram of electric double layer (EDL) next to a negatively charged solid surface.

double layer (EDL) theory in 1879 and related the electric and flow parameters for electrokinetic transport [27]. The distribution of electric charges in the immediate vicinity of the interface between two conducting phases is almost always non-uniform. Helmholtz [33] assumed that an electric tension exists at the wall-liquid surface, which generates an electrical double layer. This he treated with the electrostatic laws of capacitors combined with hydrodynamics. Figure 3.2 details all the main parameters describing an EDL. The EDL can be divided into two distinct zones; the stern layer and

the diffuse layer, which are separated by a shear plane. The stern layer is immediately next to the charged dielectric surface and is formed due to strong attraction of ions in the fluid to the oppositely charged wall surface.

These immobilized ions shield the surface electric potential ψ_o leading to a greatly reduced potential at the end of the stern layer known as the zeta potential ζ. The distance from wall, where the electrokinetic potential energy is equal to the thermal energy in known as debye length λ_D. Zeta potential and ionic concentration govern electrokinetic transport in the EDL. Electroosmotic mobility is proportional to zeta potential, while ion concentration determines the thickness of EDL. Dutta and Beskok [34] have also shown that the effect of charge distribution described by electrokinetic potential is felt beyond the debye length λ_D. There is a steep decline in the potential and at around 4.5 λ_D it drops to about 1% of its original zeta potential.

The EDL leads to electrokinetic effects, which can be divided into four categories (Probstein, 1994) [35] as follows:

- *Electroosmosis:* Motion of ionized liquid relative to the stationary charged surface by an applied electric field.

- *Electrophoresis:* Motion of the charged surface relative to the stationary liquid by an applied electric field.

- *Streaming Potential:* Electric field created by the motion of ionized fluid along stationary charged surfaces.

- *Sedimentation Potential:* Electric field created by the motion of charged particles relative to a stationary liquid.

In essence, if an electric field is applied to a fluid with an electric double layer, the ions within the fluid will feel a Coulomb force, charge migration will occur, and fluid will be dragged along with the charges creating a net flow.

Electroosmosis has been used for chemistry applications since the late 1930's [36]. Unlike direct actuation of conducting drops, electroosmosis does not rely on the direct forces being exerted upon a fluid by an applied electric field. Rather electroosmosis relies upon the presence of an EDL that forms when an ionized solution interacts with static charges on the surface of a dielectric material. According to Pauli, electroosmotic phenomena, like any other electrokinetic phenomena, may be interpreted by the same theory of dissociation, which has been so fruitful in the study of colloids [36]. It can be assumed that ionogenic complexes exist at the fixed surface similar to those existing on colloidal particles. These complexes dissociate electrolytically and confer an electrical charge on the walls, whilst a charge of opposite sign goes in to the solution in the form of counter-ions; these are distributed with their greatest density near to the walls and decreasing density with increasing distance. In this way, the electrochemical double layer is formed and the actual electric tension arises.

This is well shown by the movement of liquid with respect to walls under the action of an electric field. The electric field acts on counter-ions forcing them to migrate towards the oppositely charged electrode. These counter ions, due to their hydration and viscosity of the liquid, draw a certain amount of bulk fluid along with them and thus move it with respect to the walls. In essence, if an electric field is applied to a fluid with an electric double layer, the ions within the fluid will feel a Coulomb force, charge

migration will occur, and fluid will be dragged along with the charges creating a net flow.

Although electroosmosis is an attractive technique for micro-fluidic pumping, it is not desired in the present application since the device operates on capillary electrophoresis, where electroosmotic action needs to be suppressed. Experiments preformed indicate a strong dependence of fluid velocity and dispersion rate on the surface charge distribution. Herr et al. [37] have used various surface materials as well as polymeric coatings to obtain different surface charge distribution by modifying the local zeta potential. McClain et al. [38] were able to detect *Escherichia coli* (*E. coli*) using pure electrophoretic transport. They used poly-dimethylacrylamide (PMMA) for suppressing electroosmosis. Schasfoort et al. [39] have used embedded surface electrodes to locally alter the zeta potential. They built micro-channels using conducting material, and have covered these with a thin layer of insulator. It was shown that electroosmotic flow velocity can be altered by applying electrostatic potential on the walls.

Electrophoresis is the process of inducing motion of charged particles relative to a stationary liquid using an applied electric field, where the liquid acts as a conducting medium. The forces acting on the particle are, Columbic forces due to the net particle charge in an electric field, and an opposing viscous drag. The velocity at which the charged particle moves towards the anode or cathode is known as the electrophoretic migration velocity. This velocity is directly proportional to the applied electric field and
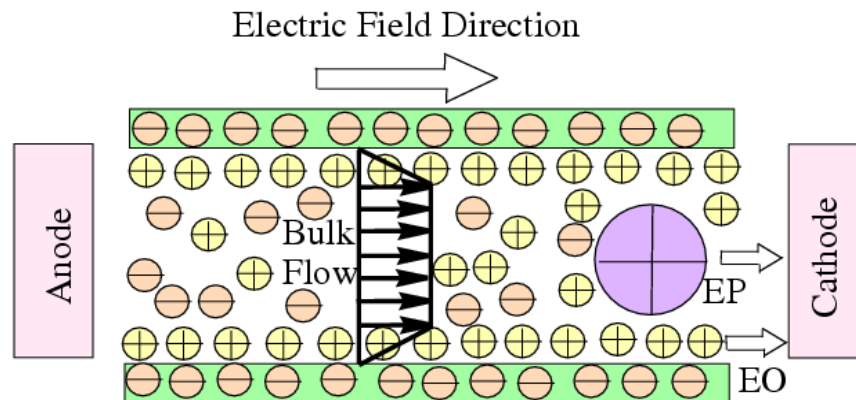
FIGURE 3.3: Schematic of bulk flow due to combined electroosmosis and electrophoresis in a microchannel with an electric field along its length.

net charge of the particle; and is inversely proportional to the viscosity of the particle and its size.

Electrophoresis is a separation method and is widely used in the field of biochemistry, where purification of labile substances from biological material is a problem often encountered. Electrophoresis technique can be easily automated to get fast analysis times. Cabrera et al. [40, 41] have extensively used isoelectric focusing and electrophoresis for separation of proteins and bacterial cells etc.

The phenomenon of electrophoresis and electroosmosis are illustrated in Figure 3.3. The microchannel is filled with ionic fluid inside and has dielectric walls having a negative zeta potential. Since the wall surface is negatively charged, a stern layer dominated by cations is formed. These cations tend to move towards the cathode and in the process, drag the bulk of flow along with them. At the same time, positively charged species in the bulk of fluid, experience electrostatic attraction towards the cathode

(electrophoresis). The resulting electrokinetic mobility μ_{ek} includes both electroosmotic and electrophoretic effects [42,43]. Mobility is related to the electrokinetic migration velocity $\vec{u}_{ek}$ and applied electric field $\vec{E}$ by:

$$\vec{u}_{ek} = \mu_{ek}\vec{E}$$

The electroosmotic mobility for infinitesimally thin EDL is given by Helmholtz-Smoluchowski relation [44]:

$$\vec{u}_{eo} = -\frac{\zeta\varepsilon}{\mu},$$

where ζ is the zeta potential. Using the electroosmotic mobility, we obtain the Helmholtz-Smoluchowski electroosmotic velocity u_{eo}

$$\vec{u}_{eo} = \mu_{eo}\vec{E} = -\frac{\zeta\varepsilon}{\mu}\vec{E}.$$

Negative sign arises due to the sign of surface zeta potential. A typical velocity profile for flow due to electroosmosis, in a microchannel is shown in Figure 3.3. electrophoretic mobility due to Columbic forces is given by

$$\vec{u}_{ep} = -\frac{2\zeta\varepsilon}{3\mu},$$

where the 2/3 coefficient is appropriate for particles. This results in electrophoretic migration velocity of

$$\vec{u}_{ep} = \mu_{ep}\vec{E}.$$

3.4   ELECTROPHORETIC MOBILITY OF COMMON BACTERIA

Electrophoretic mobility for particles is mostly determined experimentally [44]. Studies at EFS Lab have shown that bacteria and viruses are negatively charged in the pH ranges of drinking water [45]. Effects of pH and mineral content of water on the transport of bacteriophages have also been conducted [46]. Since mobility of bacteria is a critical design parameter, it is important to quantify the electrophoretic mobility of some common bacteria. The dependence of electrophoretic mobility on the starvation condition of bacteria is also studied. Capillary electrophoresis is used to find out the electrophoretic mobility values. The lowest electrophoretic mobility value of all the bacteria should be used to determine the time scale for the capture of bacteria in the device design. This ensures that the design is generic to all the bacteria types.

Electrophoretic mobility of various bacteria were determined using capillary electrophoresis equipment (Beckman P/ACE 5500). Drinking water was used as the suspension media in place of buffers that are commonly used. Bacteria were grown in four different conditions, "rich", "minimal", "starved" and "dead". A brief description of how these conditions were created is given in Table 3.2.

These samples are then suspended in drinking water and the electrophoretic mobility for each starvation condition determined using the capillary electrophoresis equipment. That gives an idea of variation in electrophoretic mobility of bacteria with starvation condition. As already mentioned, these electrophoretic mobility values will be used in designing the capture and concentration device. The next phase is to fabricate a device based on the design outline, test it and quantify the results.

TABLE 3.2: Description of growth media

"Rich media"	LB medium → washed → suspended in water
"Starved cells"	LB medium → washed → 4°C for 15 days
"Minimal media"	Minimal medium → washed → suspended in water
"Dead cells"	LB medium → 1 % Sodium azide for 2 days Ionizing Radiation (4 kGy)

CHAPTER IV

PHASE III: DESIGN EMBODIMENT

4.1 EXPERIMENTAL SETUP

The experimental setup consists of four main components:

(i)   Fluorescence microscope and image acquisition system

(ii)   Prototype microfluidic device for the capture of bacteria

(iii)   Microsystem with syringe pump, power supply and multimeters and

(iv)   Bacterial testing and quantification setup

Figure 4.1 shows the first, second and third components of experimental setup. They are located in the Biomicrofluidics Laboratory in the Department of Mechanical Engineering, Texas A&M University. Bacterial testing and quantification is being done in collaboration with the 'Environmental and Food Safety Lab' in the Department of Poultry Science, Texas A&M University.

The microsystem comprising of syringe pump, power supply unit and multimeter constitutes the flow input, power supply and current monitoring equipment. A constant, pulse free flow is supplied to the microfluidic device using a micro syringe pump. Output from the prototype device is collected into vials that are sent for analysis. The microfluidic device is mounted on stage of the fluorescence microscopy system if qualitative analysis about bacterial adhesion is to be done, else it can be used as a black box.
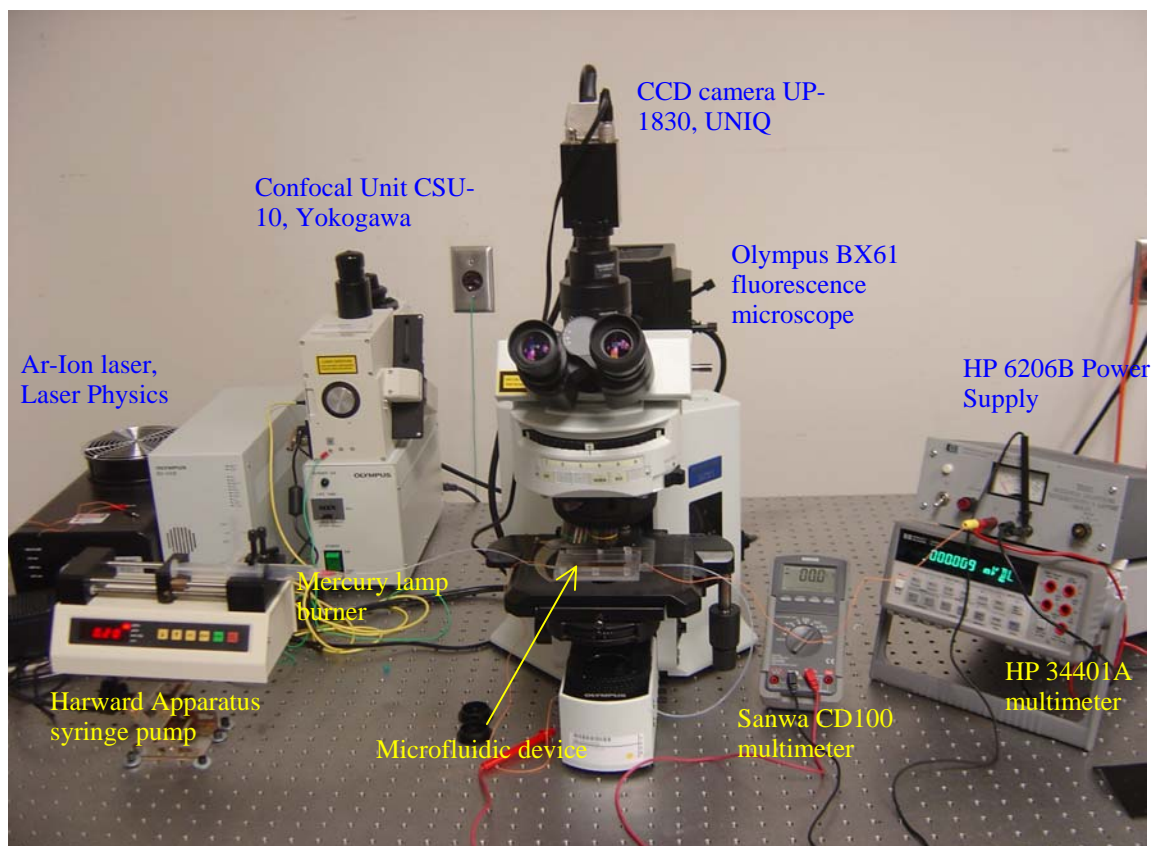
FIGURE 4.1: Experimental setup consisting of fluorescence microscope, image acquisition system, syringe pump, power supply & multimeter.

The image acquisition system allows us to capture images of bacteria at various locations of the microfluidic device. This helps us in understanding the characteristics of bacterial adhesion. Current flow through the microfluidic device and the potential applied across it are monitored using multimeters. Current flow through the device is also measured to ensure continuity in the circuit. Any undue fluctuations in current are an indication that something is wrong in the device. Bacterial cultures are grown in the Environmental and Food Safety (EFS) Laboratory. These cultures are suspended in the

desired medium and different dilutions are prepared freshly before every experiment. Once the experiment is over, samples collected are sent for analysis back to the EFS laboratory. Bacterial culture methods are then used for quantification.

4.2   DESCRIPTION OF APPARATUS

4.2.1   Fluorescence microscope and image acquisition system

Fluorescence microscopy is used to image bacteria. The fluorescence microscopy unit is made up of the following three systems:

i)   Reflected fluorescence system

ii)   Motorized microscope system

iii)   Control box system

An image acquisition system is coupled to the fluorescence microscopy unit above to complete the qualitative study setup.

The reflected fluorescence system consists of Power Supply Unit, Mercury Lamp Housing, ND Filters and Fluorescence Mirror Unit. A power supply unit (BH2-RFL-T3) powers the mercury burner (Olympus USH102D, 19V, 100W), which is housed in a mercury lamp housing (Olympus U-LH100HG). Blue light at wavelength of 488 nm, emitted by the burner is used to excite the fluorescent specimen. An appropriate set of mirrors and filters is used to get a clear image. Since the excitation light belongs to the Indigo-Blue (IB) range, the mirror unit U-MNIB2 (Universal – Mirror - Narrow Bandwidth – Indigo Blue Excitation – Model 2) is used. The filter cube consists of a BP470-490 excitation filter (Band Pass 470 – 490 nm), a Barrier Filter BA510IF (Barrier Filter 510 nm) and a DM570 (Dichroic Mirror 570 nm). ND Filters U-25ND6 and U-25ND25 are used to adjust the transmitted light intensity. They are more commonly

referred to as neutral and heat density filters. The bacteria are made to fluoresce by tagging them either with green fluorescent protein (GFP) or BacLight® dye (Molecular Probes).

The reflected fluorescence system described above is mounted onto an Olympus BX-61 motorized system and wired to a control box system to complete the microscopy setup. A high speed CCD camera (XR mega 10, UNIQ UP-1830, Stanford Photonics limited) with a maximum frame rate of 30 fps is used to capture the videos and snapshots. Four different objectives with magnifications of 10X, 20X, 40X and a long working distance 60X with numerical apertures of 0.45, 0.50, 0.55 and 0.75 respectively are used to capture the light emitted from the sample. The 60X long working distance objective can image through aqueous medium (2 mm thickness in our case) to focus on the bottom electrode surface. The objective can be adjusted to varying cover slip thickness using a correction collar. This gives a better resolution image compared to the other objectives. As the magnification of the objective increases, the view window reduces since we are looking at a magnified view of a smaller area in the same view window. QED Imaging software, developed by Media Cybernetics, Silver Spring, MD is used to analyze the images, make videos and take snapshots.

20x objective is the default objective for regular observation of the channel and to generate videos showing capture and release. This magnification also allows the observation of entire channel width in one window. Higher magnifications up to 60x can be used to narrow down onto a couple of bacteria and see their mutual interaction or with the electrode surface. All the objectives were corrected to a glass slide of thickness

0.15mm. The area of focus using the different objectives, as given by the user manual are as follows:

Objective	Area of focus
10 X	660 µm x 660 µm
20 X	330 µm x 330 µm
40 X	165 µm x 165 µm
60 X	82.5 µm x 82.5 µm

QED imaging is an image capturing software compatible with the CCD camera and the motorized microscopy system. It is used to capture still shots and videos of the device in working and to operate the motorized microscopy system. The videos and snapshots are stored as raw data files that are later on processed to create movies using "Virtualdub" software. Images and snapshots captured by the camera may need to be processed using imaging software like Adobe Photoshop to correct their contrast and sharpness. Rough cell counts can be made using Scion Image (NIH Image).

4.2.2   Prototype microfluidic device for showing proof of concept

A preliminary prototype device was designed for showing the proof of concept using the standard fluorescent microscopy unit by imaging through the device. This will give an idea of the critical design parameters that influence bacterial adhesion. Initial studies without any flow were conducted using this device. As seen in the Figure 4.2, construction of the device is very simple. A test channel is created by sandwiching a PDMS spacer between two Indium Tin Oxide (ITO) electrodes (Delta Technologies
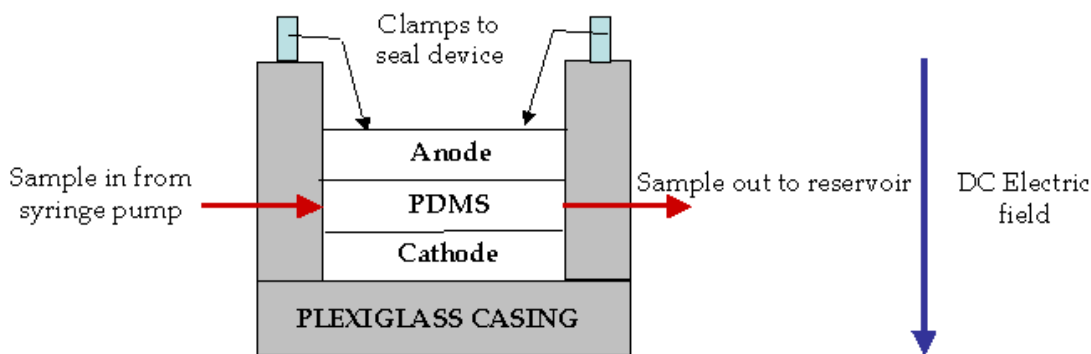
FIGURE 4.2: Schematic of prototype for showing proof of concept.

Ltd., MN). ITO is a transparent conducting material and facilitates imaging. The PDMS spacer is created from a custom made mold and also forms the channel. Thickness of the PDMS spacer determines the separation between ITO electrodes; in this case it is 2 mm. Further, clamps are used to press down the top electrode to seal the device and prevent any leaks. The plexiglas casing and mold for PDMS are all machined using micro CNC machining facility at Texas A&M University. The picture of the assembled device is shown in Figure 4.3. Solid models of the plexiglas casing, PDMS mold and L-clamps are included in Appendix.

4.2.3   Modified prototype device for qualitative/quantitative testing

A second prototype was fabricated based upon the observations made in the first prototype. This new design also included the results given by optimization routines. The microfluidic device was fabricated using plexiglas. All the components were manufactured using micro CNC machines. 3D models of the components were first made using SolidWorks 2004®. These SolidWorks files were then converted to part
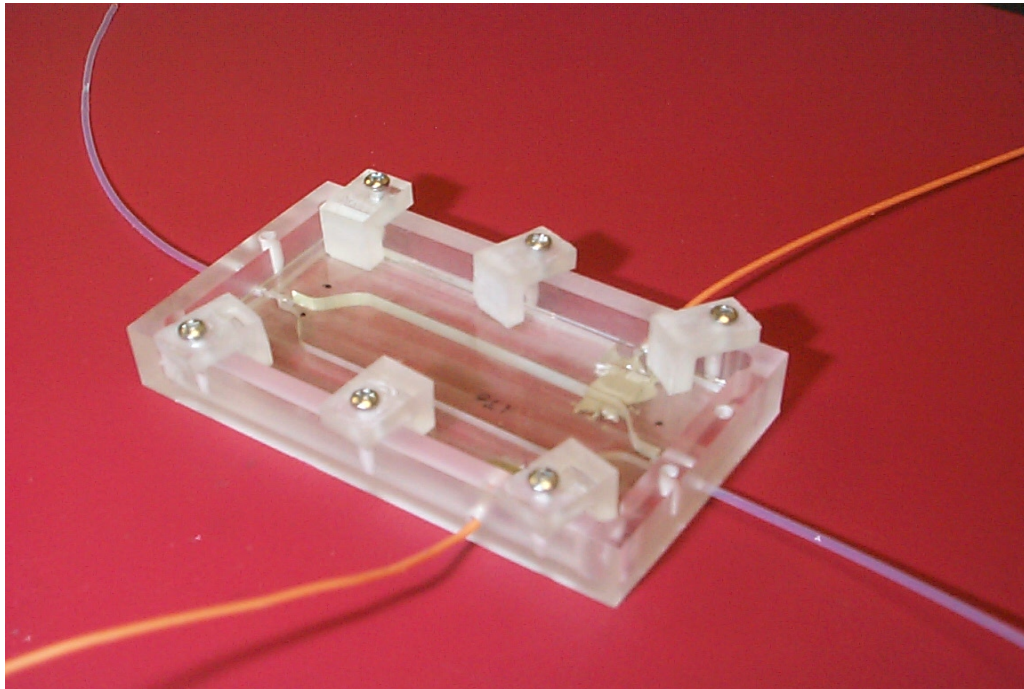
FIGURE 4.3: Assembled prototype device for showing proof of concept.

programs before being input to the micro CNC milling machine (Haas Automation, Inc.,

Oxnard, CA). For other parts like the electrodes, CNC milling machine (Haas

Automation, Inc.) was used. On the micro-milling machine, a vacuum chuck was used to

hold the specimen in place while a custom made faceplate was used on the Haas milling

machine since the size of stock from which electrodes were fabricated was small.

Electrodes were made from copper because it is easily machined and one can

achieve a smooth finish on it. Being an active metal, copper reacts electrochemically

when it is in contact with water on applying an electric potential as low as 0.5 V. So it is

essential that the copper surface be isolated from buffer solution to prevent any type of

electrochemical reactions. This can be achieved by coating the electrodes with a thin layer of gold of around half a micron thick using Physical Vapor Deposition (PVD). Gold coating adhered strongly and was not removed unless it was ground off the surface by polishing it. Copper bar was precisely rolled (Haas Automation, Inc.) down to the desired thickness, in our case 2.5mm. This formed the raw material that was then machined on CNC milling machine to the required geometry. The machined components had to be free of burrs and other surface deformations. Good finish was achieved by setting a low material removal rate and increasing the number of passes for removing the material. This removes all the burrs and other surface features that would cause non-uniform electric fields. Adequate tolerance was given so that the machined components could be polished to mirror finish. On observation under microscope (Nikon), it was seen that the surface had features in excess of 10 microns. This was undesirable since the electrode surface would be uneven and unfit for coating with protective layers. Electrodes were polished using Buehler grinder, starting with a polishing paper grade of 1000 and up. Final mirror finish was achieved by using alumina powder of 5-micron grade for polishing. Inspection of the electrode after polishing showed that the surface features were sub micron in size.

Though the adhesion strength gold layer coated by PVD (BOC Edwards Auto 306 Metal Evaporation Chamber) is good, the layer is typically porous. This leads to interdiffusion with copper, which will affect its performance very shortly after immersion in buffers. The general way to overcome this problem is to add a diffusion barrier layer of nickel or palladium between copper and gold. That will give certain dependability of electrode for testing - i.e. we can be sure that we will be reading the

gold electrode reaction with the chemicals in the device, without interference from copper. Gold was chosen since it is a noble metal and has a high electrode potential compared to other materials. This prevents it from getting into any kind of electrochemical reaction with the water or the buffer flowing in device. By any method, chances are that gold electrode will not be good for long unless quite a thick deposit over 2 microns is made, preferably by electroplating. Physical vapor deposition was used because it gives a strong and uniform coating on conducting materials and non-conducting surfaces (silica glass, plexiglas) alike.

The sample to be coated is first cleaned with acetone and ethyl alcohol to remove grease. It is then fixed to a rotating sample holder to get uniform thickness of gold coating, either by using a clamp or a double-sided tape. Care must be taken to ensure that the samples are placed close to the center of the plate and firmly stuck to get a better coating and to prevent them from falling down. Once the samples are in place, the vacuum bell jar is removed carefully and the metal to be coated is put into boats (small cups with long handles on either side) that are fixed to electrical contacts using screws. The boats are made of metals like tungsten or molybdenum that have high melting point and resistance, so that they do not melt even after reaching temperatures at which the metal to be coated starts boiling and becomes incandescent. Once everything is in place, the bell jar is cleaned to remove traces of grease and oil on it and then placed carefully back around the equipment. High vacuum grease is then applied to the rubber sealing on either ends of the bell jar and the top cover (holding the samples) is brought back to place. The vacuum pump is then started to degasify this enclosure. Vacuum serves two purposes; firstly it prevents oxidation of the metal to be coated at high temperatures
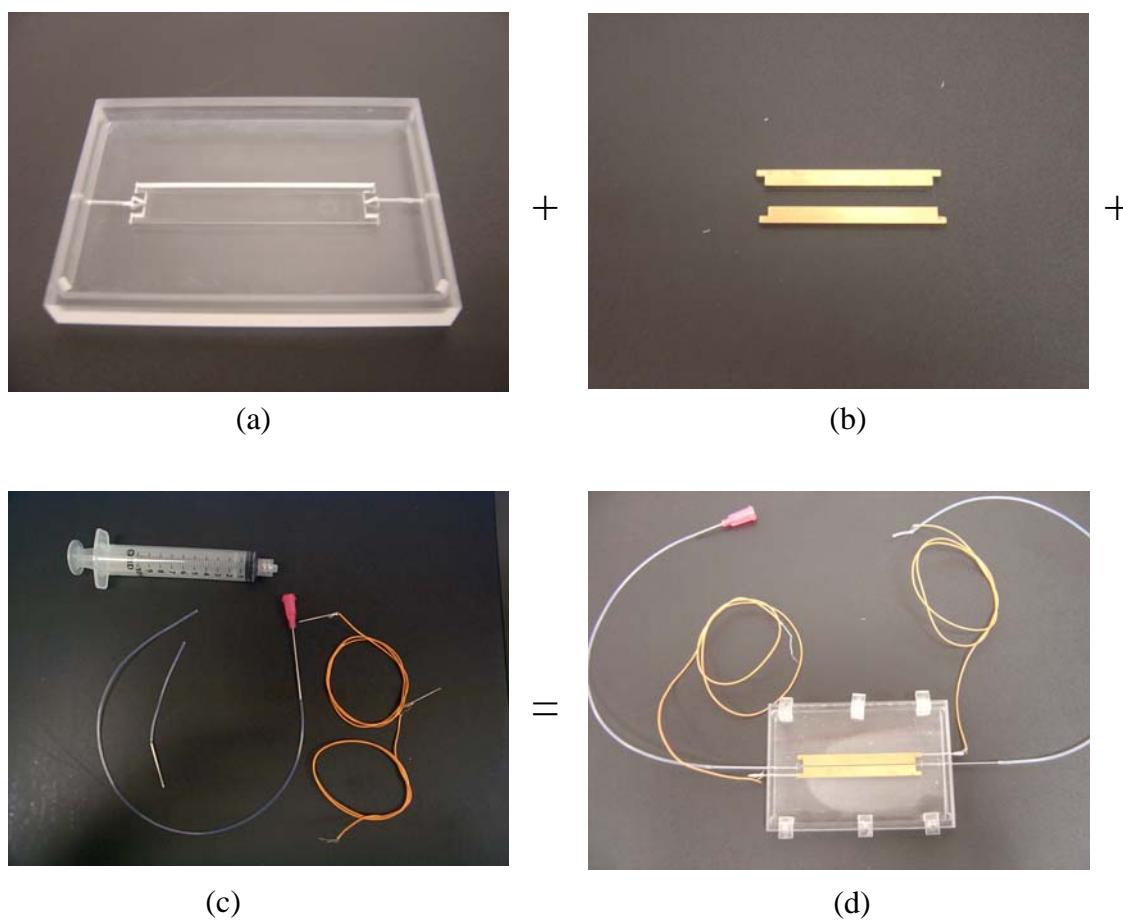
FIGURE 4.4: Assembly of new prototype device. (a) Plexiglas base with groves to align electrodes; (b) Copper electrodes coated with a gold layer to eliminate electrochemistry; (c) Electrical connections, inlet and outlet tubing and syringe; (d) Assembled device.

since it is in molten state when it is being coated. Secondly it also protects the sample that is to be coated from excessive heat because it eliminates convection heat transfer. Using this method it is possible to coat gold onto materials like glass or even plexiglas.

The chamber takes 4 to 6 hours to reach a vacuum of around 10^{-6} torr, after which the actual metal deposition process is started. Once suitable vacuum is reached, the sample holder is uniformly rotated using a motor and simultaneously current is very slowly increased to heat the boat. When current reaches between 4 to 5 amps, we see that the metal to be coated starts to boil inside the boat. We then open the shutter and leave it there till the desired thickness of coating is achieved. Precaution should be taken to ensure that pressure inside the vacuum chamber does not go above 2×10^{-5} torr, so as to get a consistent coating quality. Once the desired thickness is achieved, the shutter is closed, current is slowly brought down to zero and the sample holder rotation is stopped. The chamber is left to cool down to room temperature for an hour and then vacuum is released. Once the work is over, the chamber is again set to pump down to vacuum.

Figure 4.4 shows the assembled prototype device. The main components that go into the assembly are: Plexiglas base, gold plated electrodes, inlet and outlet connectors and tubing, the power connectors for electrodes and the top cover slip to cover the channel from top. Leakage is avoided by using PDMS between the cover glass and electrodes. As seen in the figure, the device has been made is such a way that it can be completely disassembled for cleaning and put back together very quickly. A spacing of 250 microns is maintained between electrodes by fabricating them such that they are exactly 250 microns shorter than the separation between the aligning grooves. Solid models of all the other components making up the device are given included in Appendix.

TABLE 4.1: Nominal min/max flow rates with diameter

Nominal Syringe Size	Nominal Diameter (mm)	Flow Rate (ml/hr)	
		Min	Max
1 ml	4.61	0.01	1.13
2 ml	7.28	0.01	4.14
3 ml	8.66	0.101	3.73
5 ml	10.3	0.05	7.20
10 ml	14.57	0.05	10.40

4.2.4   Microsystem with syringe pump, power supply and multimeters

This set of equipment is used to monitor and control the flow of sample, current etc. It consists of Syringe Pump, Power supply and Multimeters.

a) *Syringe Pump:* It is used to supply constant flow rate of sample to the device. The sample to be pumped is loaded into a standard syringe. The syringe plunger is pushed at a speed determined by the flow rate to be delivered and the syringe size being used. Pulse free flow is achieved using standard infusion pump (Harvard Apparatus Pump 11 plus). For a particular syringe volume and diameter, there is a minimum and maximum flow rate that the instrument can deliver. To get the required flow rate, one has to choose the appropriate syringe diameter and plunger motion rate. Some sample flow rates and syringe dimensions are given in the Table 4.1.

b) *Power Supply:* A Hewlett Packard 6206B variable voltage DC power supply (0-30 V at 0.5 amps; 0-60 V at 1 amp) was used to apply the electric field across the electrodes. The power supply had a coarse setting and a fine setting allowing to accurately set a voltage up to the third decimal value. When current control was

required, Kepco power supply (ATE36 – 1.5M, 0-36V, 0-1.5 amps) was used since it even had a current control apart from voltage control. At all times the voltage used was kept low to avoid electrochemistry related complications.

c) *Multimeters:* Digital multimeters were used to monitor voltage and current variations in the circuit. Voltmeter was connected across the device while ammeter was connected in series with the device. One of the multimeters was a Hewlett Packard 34401A multimeter with a least count of 0.001 milli volts, while the other one was a Sanwa CD100 multimeter with a least count of 0.01 micro amps and 0.1 milli volts.

4.2.5   Miscellaneous

Many other components were used apart from the main setup. Some of the important ones are discussed briefly below.

a) *Chemical Reagents:* Organic solvents like ethyl alcohol, iso-propyl alcohol and acetone were used as cleaning reagents. The device was designed in a way that it could be completely disassembled and cleaned. This makes it reusable unlike many other microfluidic devices that are made for a single use only. The device is thoroughly sonicated in cleaning reagents after every use, to wash off all the bacteria and other contaminants. Occasionally dilute aqua regia (mixture of hydrochloric acid and nitric acid) and acetic acid were used to clean off scale and other sediments from the device

b) *PDMS:* Polydimethylsiloxane (PDMS) was used to seal the device from any leakages. It is an elastomer that can be molded to take any shape on curing. PDMS components are made using specially fabricated molds. The base and hardener are mixed in 10:1 ratio by weight, poured to into a mold and left to set in an oven at around 60°C for 6 hours. Other shapes can be made using PDMS by changing the shape of mold.

c) *Conducting Epoxy:* Silver epoxy (Stan Rubenstein Associates) was used to get better contact between the different electrical components and also as an adhesive, to adhere electrodes and their contacts. Regular epoxy was also occasionally used wherever needed.

d) *EOF Flow Suppression:* EOF flow due to cover glass is suppressed by flowing a 4% by weight solution of methyl cellulose (TCI America, Portland) in the channel for a couple of hours [47]. This is then flushed out with distilled water for a few channel volumes, followed by ethyl alcohol and distilled water again for disinfecting and rinsing purposes respectively. Actual flow of bacterial sample is then started. EOF can also be suppressed by using a material that has very low zeta potential. Plexiglas (PMMA, Polymethylmethacrylate) does not contain a pH ionizable function groups arising from deprotonation of silanol groups, unlike glass or fused silica. So, plexiglas displays a significantly smaller EOF compared to silica glass, especially at high pH values [48, 49]. Even PDMS has been used by researchers in situations where EOF flow needs to be suppressed.

e) *Softwares:* MATLAB was used for optimization of the channel dimensions. The "Optimization Toolbox" in MATLAB was employed for this purpose. Multi objective optimization of non-linear objective functions was carried out. The optimized geometry values will be used in the fabrication of the final device once the prototype device is tested for efficient operation. Many other softwares were used for image capture and processing. Some of them are: QED Imaging, Adobe Photoshop, Scion Imaging and Virtual dub.

f) *Miscellaneous:* Miscellaneous other components like syringes, pipettes, hand gloves, needles, tubing, screws, drilling and tapping set were all used where required. Most of these small things were purchased from Small Parts Inc., Florida.

g) *Bacteria Culture and Analysis:* Both bacterial culture and analysis was done at the Environmental and Food Safety Laboratory (EFS). Bacteria samples were freshly prepared from the main culture for each experiment. Since the device had to be generic, we used common pathogens like *E. coli, Salmonella, Pseudomonas* and less common bacteria like *Klebsiella.* The bacteria were tagged with Baclight® dye since fluorescence microscopy was used for imaging. Once tagged, these bacteria are suspended in the desired medium and different dilutions are prepared for testing in the microfluidic device. Experiments are conducted in Biomicrofluidics lab and the samples collected are taken back to the EFS lab for analysis and cell counts. Analysis of these samples gives us the concentration of bacteria after the sample is passed through the capture and concentration device. Comparison of the bacterial concentration of samples before and after passing them through the capture and concentration device determines its capture efficiency.

4.3 EXPERIMENTAL PROCEDURE

The microfluidic device is fabricated for reuse, and so it has to be cleaned and assembled after every experiment. To assemble the device, electrodes are snapped into their grooves and sample inlet/outlet and electrical contacts are made. The device is then sealed off from the top with a cover slide to complete the channel. Using a cover slip also enables microscopy and imaging of the channel. This completes the device assembly section. A voltmeter is connected in parallel to the device to read out potential

drop across the device and an ammeter is connected in series to measure current flow through the system as a function of time.

Before working on anything, the whole workplace is cleaned with acetone, iso propanol and then disinfected with 200 proof ethyl alcohol. The microfluidic device is then assembled and checked for electrical continuity and absence of any leakages. It is first flushed with 200 proof ethyl alcohol for 5 min and then with de-ionized water for 15 min to sterilize the device and rinse off all the ethyl alcohol respectively. Simultaneously the microscopy unit is turned on and fluorescence lamp allowed to reach the working brightness (~ 10 min).

Once the device is setup, image acquisition system is also readied. Now the assembled device is set on stage and the channel is brought into the focus of microscope. The device is first flushed with 200 proof ethyl alcohol for 15 min at a high flow rate, followed by deionized water for an equal amount of time. This completely disinfects the system and the inlet and outlet tubing. The bacterial sample is then started to run through it and allowed to run through the system for 15 more minutes at a high flow rate. Electric field is then started and no sample is collected for the first 30 minutes so as to allow all the outlet tubing to be replaced with sample from the device. After this output flow is regularly sampled into microtubes to observe changes in bacteria numbers with time. These samples were sent to the bacteria testing and quantification lab (EFS lab) for further analysis that would determine the effectiveness of our device and also identify the parameters affecting its performance. Analysis of these samples gives us the concentration of bacteria after the sample is passed through the capture and concentration device. Comparison of the bacterial concentration in samples before and

after passing them through the capture and concentration device determines its capture efficiency.

4.4   OPTIMIZATION OF THE ORIGINAL PROTOTYPE

As mentioned earlier, this device is being developed mainly to serve the future needs of NASA; specifically to capture and concentrate microbes from a limited supply of recycled water on long term manned space missions. It goes without saying that the device should be compact, should be light in weight and must be energy efficient if it has to cater well to the needs of NASA. As outlined in the design philosophy of IIDE, optimization of the device comes after building and testing of a prototype device. The proof of concept is demonstrated using the prototype and observations made using the prototype device are addressed. The parameters that need to be optimized are considered in building an improved prototype and ultimately in construction of the final device that will be delivered.

Reducing the volume automatically reduces weight of the device since we are indirectly reducing the amount of material needed for fabrication. But as we keep scaling down the device dimensions, its surface area to volume ratio increases substantially. This increases the hydraulic power consumption of the device. A little consideration shows that the two objectives above are opposing and so there should definitely be a point where both these functions are satisfied optimally. This kind of a problem with two opposing functions is also one of the most common optimization problems in calculus. It is a typical maxima/minima problem where we are extremizing a function, but it is often difficult to find a closed form for the function that must be extremized. Such difficulties arise when one wishes to minimize or maximize a function subject to certain outside

conditions or constraints. Thus the optimization problem calls for a more thorough mathematical treatment.

4.4.1 Optimization techniques

Various techniques available for solving optimization problems of the kind we just discussed are [50]:

1. Mathematical programming techniques

2. Stochastic process techniques and

3. Statistical methods.

Mathematical programming techniques are useful in finding the maximum/minimum of a function with several variables and numerous constraints. Stochastic process techniques can be used to analyze problems described by a set of random variables having known probability distributions. Statistical methods enable one to analyze the experimental data and build empirical methods to obtain the most accurate representation of the physical situation. Mathematical programming techniques are used for the current problem since they are suitable for solving engineering design problems [51, 52].

Newton, Lagrange and Cauchy developed the first mathematical programming techniques. Newton and Leibnitz developed calculus methods, while Bernoulli, Euler, Lagrange and Weirstrass contributed to the calculus of variations and minimization of functionals [50]. They are categorized under "Classical Optimization" methods of differential calculus, which are used to find the unconstrained maxima and minima of a function of several variables. These methods assume that the function is differentiable twice with respect to the design variables and that the derivatives are continuous. Later

on, a method for constrained optimization by adding unknown multipliers was developed by Lagrange. For problems with equality constraints, we apply the Kuhn-Tucker conditions, to identify the optimum point. But these methods lead to a set of nonlinear simultaneous equations that may be difficult to solve analytically. So numerical methods are used to solve nonlinear problems, wherein the approximate solution is sought by proceeding in an iterative manner by starting from an initial solution.

In constrained optimization, the given problem is transformed into an easier sub-problem that can then be solved and used as the basis of an iterative process. The usual procedure is to translate the constrained problem to a basic unconstrained problem by using a penalty function for constraints that are near or beyond the constraint boundary. In this way the constrained problem is solved using a sequence of parameterized unconstrained optimizations, which in the limit (of the sequence) converge to the constrained problem. These methods are now considered relatively inefficient and have been replaced by methods that have focused on the solution of the Kuhn-Tucker (KT) equations [53]. The Kuhn-Tucker equations are necessary conditions for optimality for a constrained optimization problem. If the functions to be optimized are convex functions, then KT equations are both necessary and sufficient for a global solution point.

4.4.2   Lagrange multipliers theory

The method of Lagrange multipliers is a powerful tool for solving our problem without the need to explicitly solve the conditions and use them to eliminate extra variables. Using Lagrangian multipliers technique, we can analytically solve for optimal solution if the constraints are all linearly independent functions of the variables.

Lagrange multipliers technique stands out uniquely due to its simplicity in concept and ability to solve nonlinear optimization functions with nonlinear constraints. Doing multi-objective optimization is also relatively simple with this method. But we have to use iterative methods if we have to solve problems with nonlinear constraints.

The basic theory of Lagrange multiplier method is given initially for a simple problem of two variables with one constraint. This method can be extended to a general problem of n variables with m constraints in a similar fashion. Consider the problem of minimizing a function:

$$\text{Minimize } f(x_1, x_2) \qquad (4.1)$$

Subject to

$$g(x_1, x_2) = 0 \qquad (4.2)$$

A necessary condition for f to have a minimum at some point $f(x_1^*, x_2^*)$ is that the total derivative of $f(x_1^*, x_2^*)$ with respect to x_1 must be zero at (x_1, x_2). By setting the total differential of $f(x_1, x_2)$ equal to zero, we obtain

$$df = \frac{\partial f}{\partial x_1} dx_1 + \frac{\partial f}{\partial x_2} dx_2 = 0 \qquad (4.3)$$

Since $g(x_1^*, x_2^*) = 0$ at the maximum point, any variations dx_1 and dx_2 taken about the point (x_1^*, x_2^*) are called admissible variations provided that the new point lies on the constraint:

$$g(x_1^* + dx_1, dx_2^* + dx_2) = 0 \qquad (4.4)$$

The Taylor's series expansion of the function in Eq. (4.4) about the point (x_1^*, x_2^*) gives

$$g(x_1^* + dx_1, dx_2^* + dx_2) \approx g(x_1^*, x_2^*) + \frac{\partial g}{\partial x_1}(x_1^*, x_2^*)dx_1 + \frac{\partial g}{\partial x_2}(x_1^*, x_2^*)dx_2 = 0 \qquad (4.5)$$

Where dx_1 and dx_2 are assumed to be small. Since $g(x_1^*, x_2^*) = 0$, the Eq. (4.5) reduces to

$$dg = \frac{\partial g}{\partial x_1}dx_1 + \frac{\partial g}{\partial x_2}dx_2 = 0 \quad \text{at} \quad (x_1^*, x_2^*) \qquad (4.6)$$

Thus the Eq. (4.6) has to be satisfied by all admissible variations. This is illustrated in the Figure 4.5, where PQ indicates the curve at each point of which the constraints (Eq. (4.2)) are satisfied. If A is taken as the base point (x_1^*, x_2^*), the variations in x_1 and x_2 leading to points B and C are called admissible variations. On the other hand, the variations in x_1 and x_2 representing point D are not admissible since variations (dx_1, dx_2) that do not satisfy Eq. (4.6) lead to points such as D, which do not satisfy constraint equation (Eq. (4.2)).

Assuming that $\partial g / \partial x_2 \neq 0$, Eq. (4.6) can be rewritten as

$$dx_2 = -\frac{\partial g / \partial x_1}{\partial g / \partial x_2}(x_1^*, x_2^*)dx_1 \qquad (4.7)$$
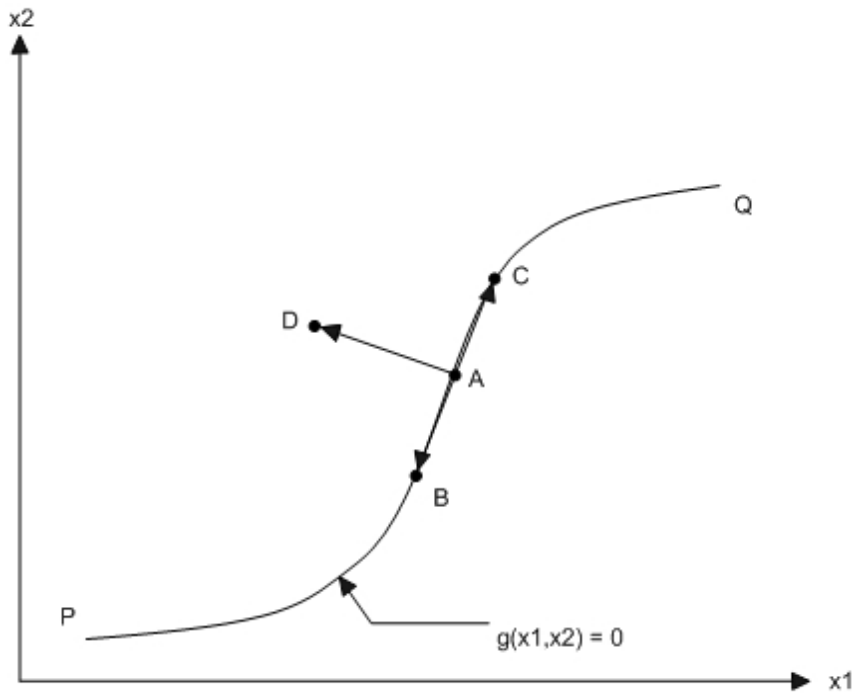
FIGURE 4.5: Variations about point A.

This relation indicates that once the variation in x_1 (dx_1) is chosen arbitrarily, the variation in x_2 (dx_2) is decided automatically in order to have dx_1 and dx_2 as a set of admissible variations. By substituting Eq. (4.7) in Eq. (4.3), we obtain

$$df = \left(\frac{\partial f}{\partial x_1} - \frac{\partial g/\partial x_1}{\partial g/\partial x_2} \frac{\partial f}{\partial x_2} \right)\Bigg|_{(x_1^*, x_2^*)} dx_1 = 0 \tag{4.8}$$

The expression on the left hand side is called the constrained variation of f. Note that Eq. (4.8) has to be satisfied for all values of dx_1. Since dx_1 can be chosen arbitrarily, that leads to

$$\left(\frac{\partial f}{\partial x_1} \frac{\partial g}{\partial x_2} - \frac{\partial f}{\partial x_2} \frac{\partial g}{\partial x_1} \right)\Bigg|_{(x_1^*, x_2^*)} = 0 \tag{4.9}$$

Eq. (4.9) represents the necessary condition for the existence of an extreme point at $X=X^*$. Eq. (4.9) can now be rewritten as

$$\left(\frac{\partial f}{\partial x_1} - \frac{\partial f/\partial x_2}{\partial g/\partial x_2} \frac{\partial g}{\partial x_1} \right)\Bigg|_{(x_1^*, x_2^*)} = 0 \tag{4.10}$$

By defining a quantity λ, called the Lagrange multiplies, as

$$\lambda = -\left(\frac{\partial f/\partial x_2}{\partial g/\partial x_2} \right)\Bigg|_{(x_1^*, x_2^*)} \tag{4.11}$$

Eq. (4.10) can be expressed as

$$\left(\frac{\partial f}{\partial x_1} + \lambda \frac{\partial g}{\partial x_1} \right)\Bigg|_{(x_1^*, x_2^*)} = 0 \tag{4.12}$$

and Eq. (4.11) can be written as

$$\left(\frac{\partial f}{\partial x_2} + \lambda \frac{\partial g}{\partial x_2} \right)\Bigg|_{(x_1^*, x_2^*)} = 0 \tag{4.13}$$

In addition, the constraint equation should also be satisfied at the extreme point, that is

$$g(x_1, x_2)\Big|_{(x_1^*, x_2^*)} = 0 \tag{4.14}$$

The last three equations (Eqs. (4.11) to (4.13)) represent the necessary conditions for the point X^* to be an extreme point.

It can be seen that the partial derivative $\partial g/\partial x_2\big|_{(x_1^*, x_2^*)}$ has to be nonzero to be able to define λ. This is because the variation in dx_2 was expressed in terms of dx_1 in the derivation of Eq. (4.10). On the other hand if we choose to express dx_1 in terms of dx_2,

we would have obtained the requirement that $\partial g/\partial x_1|_{(x_1^*,x_2^*)}$ be nonzero to define λ. Thus

the derivation of the necessary conditions by the method of Lagrange multipliers

requires that at least one of the partial derivatives of $g(x_1, x_2)$ be nonzero at an extreme

point. Introducing the Lagrange function, L can more generally represent the necessary

conditions given by Eqs. (4.12) to (4.14)

$$L(x_1, x_2, \lambda) = f(x_1, x_2) + \lambda g(x_1, x_2) \tag{4.15}$$

By treating L as a function of the three variables x_1, x_2 and λ, the necessary

conditions for extremum are given as

$$\frac{\partial L}{\partial x_1}(x_1, x_2, \lambda) = \frac{\partial f}{\partial x_1}(x_1, x_2) + \lambda \frac{\partial g}{\partial x_1}(x_1, x_2) = 0$$

$$\frac{\partial L}{\partial x_2}(x_1, x_2, \lambda) = \frac{\partial f}{\partial x_2}(x_1, x_2) + \lambda \frac{\partial g}{\partial x_2}(x_1, x_2) = 0 \tag{4.16}$$

$$\frac{\partial L}{\partial \lambda}(x_1, x_2, \lambda) = g(x_1, x_2) = 0$$

The above equations can be solved analytically for simple problems having linear

or nonlinear objective functions and linear constraints. Even multi objective functions

can be solved analytically by constructing a composite objective function with relative

weights based upon the importance of each objective, which is then solved in the usual

manner. For nonlinear optimization, we use iterative procedures to establish a direction

of search after each iteration [53]. The direction is determined using the following

methods:

- Simplex Search: These are search methods that use only function evaluations. It is used for problems that are very nonlinear or for functions that are discontinuous.

- Gradient methods: It is used when the function to be minimized is continuous in its first derivative. They use the information about the slope of the function to determine the direction of search in which the minimum can be found.

- Newton method: It is a higher order method useful when the second order information is readily available or can be easily calculated.

4.4.3 Defining the optimization problem

Any optimization problem can be split into three main parts [50]:

- Objective Function

- Design Constraints

- Design Vector

The criteria with respect to which the design is optimized, when expressed as a function of the design variables, is known as the "Objective Function". From the need statement in the previous chapter we know that the primary criteria that need to be optimized are the power and the volume of the system. Thus the two objectives for our optimization problem are: minimize power consumption of the system and minimize volume of the system. This is a Multi objective optimization problem, since we have more than one objective to be achieved while optimizing the system.

Design variables cannot be chosen arbitrarily; rather they have to satisfy certain functional and other requirements. The restrictions that must be satisfied to produce an

acceptable design are collectively called "Design Constraints". They might either be functional constraints or geometric constraints.

Certain quantities are usually fixed right at the outset and are called predefined parameters. All other quantities that are variables in the design process are called as design variables. They are usually represented in the Design Vector.

As mentioned earlier, our aim is to minimize the hydraulic power and wetted volume of the micro channels. The hydraulic power required to sustain flow in the device is given by

$$P_{ch} = \dot{Q} \times \Delta p_{ch} \qquad \text{where} \qquad (4.17)$$

P_{ch} is the hydraulic power required

$\dot{Q}$ is the volume flow rate per channel

Δp_{ch} is the pressure drop across a single channel

We assume Poiseuille flow in the channel. So the pressure drop in a single channel is:

$$\Delta p_{ch} = \frac{12 \times \dot{Q} \times \eta \times L}{W \times H^3} = \frac{12 \times Q \times \eta \times L}{n \times W \times H^3} \qquad \text{where} \qquad (4.18)$$

Q is the total volume flow rate on the device

n is the number of channels

η is the viscosity of the fluid

L is the length of the channel

W is the width of the channel

H is the height of the channel

The Volume of a single channel is given by

$$V_{ch} = L \times W \times H \qquad (4.19)$$
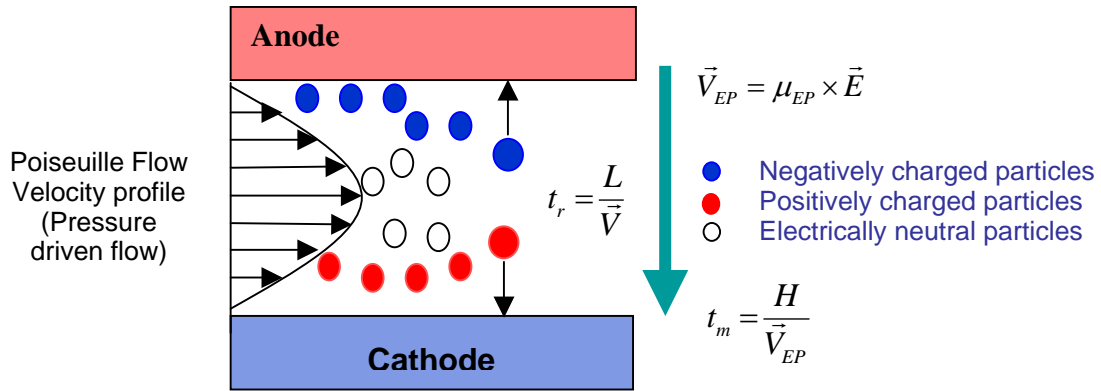
FIGURE 4.6: Illustration of mobility time and residence time.

So the wetted volume for the entire device is

$$V = n \times L \times W \times H \tag{4.20}$$

Similarly the power required for the device is

$$P = n \times P_{ch} = n \times \frac{12 \times \dot{Q}^2 \times \eta \times L}{W \times H^3} = \frac{12 \times Q^2 \times \eta \times L}{n \times W \times H^3} \tag{4.21}$$

The length, width and height of the channel are also determined by the time required by the bacteria to travel along the width of the channel while flowing in the channel under Poiseuille flow. Width of the channel should be such that the bacteria get captured at the electrode before it leaves the channel. In terms of time, the mobility time of the bacteria should be less than the residence time.

Figure 4.6 is a diagrammatic representation of the previous discussion. Expressing it in equation form:

$$t_m = \frac{H}{\vec{V}_{EP}} < t_r = \frac{L}{\vec{V}} \quad , \tag{4.22}$$

where t_r and t_m are the residence time mobility time respectively; μ_{EP} is the electrophoretic mobility, $\vec{E}$ is the electric field, $\vec{V}_{EP}$ is the electrophoretic velocity and $\vec{V}$ is the average flow velocity.

Also the height of the channel should be much smaller than its width for the Poiseuille flow assumption to hold correct.

$$W \gg H \qquad (4.23)$$

Further constraints stem from the fixed parameters like flow rate, maximum electrical potential, geometry constraints, lowest electrophoretic mobility etc.

4.4.4 Mathematical definition

The problem discussed above can be defined in mathematical terms as follows:

Objective Function: Minimize total hydraulic power and wetted volume of the device.

Design Constraints:

- Residence time should be greater than the mobility time.

- Width to height ratio should be very large for validity of 2-D Poiseuille flow assumption.

- Electric potential should be less than the 1.23V, which is the electrolysis potential of water.

Design Vector: There are some predefined parameters like volume flow rate, least electrophoretic mobility, viscosity of fluid and voltage gradient applied in a run. The variables we are left with in the design vector are the length of channel, width, height of the channel and the number of channels.

Writing it in mathematical form:

Design Vector: The predefined parameters are *Q, V, η, μ* and the design variables are *L,*

W, H and *n.* The predefined parameters can be changed for every case to get the optimal

design variables for that case. They can be written in vectorial form as

$$X = \begin{pmatrix} n \\ L \\ W \\ H \end{pmatrix} \quad \text{and} \quad P = \begin{pmatrix} Q \\ \eta \\ \mu_{EP} \\ V \end{pmatrix} \tag{4.24}$$

where X is the design vector and P is the predefined parameters vector.

Objective function:
$$Min(P) = \frac{12 \times Q^2 \times \eta \times L}{n \times W \times H^3} = f(X) \tag{4.25}$$
$$Min(V) = n \times L \times W \times H = f(X)$$

Design Constraints:

Constraint # 1:

$$t_m \le t_r \Rightarrow \frac{H}{\vec{V}_{EP}} \le \frac{L}{\vec{V}} \tag{4.26}$$

including a safety factor of 3, we rewrite Eq. (4.26) as

$$3 \times t_m \le t_r \Rightarrow \frac{3 \times H}{\vec{V}_{EP}} \le \frac{L}{\vec{V}} \tag{4.27}$$

writing Eq. (4.27) in terms of the design variables, X

$$\frac{3 \times H}{\mu \times \vec{E}_{EP}} \leq \frac{L \times A}{\dot{Q}}$$

$$\Rightarrow \frac{3 \times H^2}{\mu \times V} \leq \frac{n \times L \times W \times H}{Q}$$

$$\Rightarrow \frac{3 \times H}{\mu \times V} \leq \frac{n \times L \times W}{Q}$$

$$\Rightarrow \frac{3 \times H}{\mu \times V} - \frac{n \times L \times W}{Q} \leq 0$$

(4.28)

Constraint # 2:

The microfluidic channel is created by two parallel electrodes that are infinitely long in two of the space dimensions, and having a small separation between them. This allows us to use two-dimensional Poiseuille flow approximation given by Eq. (4.29).

$$W \gg H$$

(4.29)

Practically, we assume Poiseuille flow conditions to be satisfied when the depth of channel is more than 20 times its width. So Eq. (4.29) can be rewritten as

$$20 \times H \leq W$$
$$\Rightarrow 20 \times H - W \leq 0$$

(4.30)

Constraint # 3:

Voltage that can be applied is limited by the hydrolysis potential of water that is around 1.23V

$$V \leq 1.2$$
$$\Rightarrow V - 1.2 \leq 0$$

(4.31)

Constraint # 4:

The last constraint is called the integer and non-negativity constraint. Basically it defines which variables are non-negative and which variables cannot be fractions.

$$L, W, H, V > 0$$
$$n \in \Im$$

(4.32)

The above multi objective optimization problem can be solved directly by combining both the objectives by allocating appropriate weighting factors to the objectives given in Eq. (4.25). This gives us a single objective function as in Eq. (4.33)

$$Min(P + \alpha V) = f(X) ,$$

(4.33)

where α is the weighting factor that varies between 0 and 1. It depends on the importance we attach to the each objective. A weighting factor of 1 implies that both power and volume are equally important. If power is more important compared to volume, we decrease the weighting factor appropriately. Alternatively, both the objectives have to be combined in a way that they result in a single objective function, which can then be optimized resulting in optimized values for the design variables. Since both power and volume need to be minimized, it is much easier to minimize power per unit volume. The advantages associated with minimizing power per unit volume are:

- No need for multi objective optimization where one has to decide on how much weight to associate with each objective.
- Minimum power for any given volume can be found upon optimization.
- The objective function is independent of one variable. Length does not manifest in the objective function but reflects through constraints.

  This yields a new objective function as follows:

$$Min\left(\frac{P}{V}\right) = \frac{12 \times Q^2 \times \eta}{n^2 \times W^2 \times H^4} = f(X)$$

(4.33)

4.4.5   Matlab routines and test cases

Now that the problem is well defined, 'Optimization Toolbox' of Matlab is used for optimizing the problem. Since the given problem is a constrained nonlinear minimization problem, the function '*fmincon*' is used. The objective function is defined in a Matlab file named '*objfungrad.m*'; Design constraints are specified in '*confungrad.m*' and the design vector along with the main optimization routine to be used is written in '*optimc.m*'. These Matlab files are given in the Appendices A, B and C respectively at the end of this thesis. A guess solution is specified and the lower and upper bounds are set on design variables so that the solution is always in the bounds even if a global minima occurs at a different set design variable values. Gradient of the objective function and constraint functions are also entered in the Matlab routines to get accurate results.

Different test cases are solved by changing the design variables and effect of these variables on the optimized results is observed. Understanding the effect of each variable helps us in taking informed decisions on which design parameters can be compromised to improve our design without much loss to the overall performance of the device. Different test cases tested are given below.

CASE-I: This is the standard test case. The initial guess values for all the design variables and other constant parameters are fixed based on the requirements set by the NASA proposal.

$Q = 2 \times 10^{-6} \text{ m}^3/\text{sec};$ $\eta = 10^{-3} \text{ N.s/m}^2;$

$\mu = 3.1 \times 10^{-9} \text{ m}^2/\text{V.sec};$ $L = 0.02 \text{ m};$

V=1.0 V;   n varying from 10 to 600,

where the variables have their regular meaning.

CASE-II: In this case, the volume flow rate is increased ten times (Q = 10xQ) to see the effect of change in the volume flow rate on optimal channel dimensions. All the other variables and parameters have the same values as in the standard case (CASE-I).

CASE-III: The electrophoretic mobility of bacteria is increased ten times (μ = 10xμ). Thus the effect of varying electrophoretic mobility can be seen. All the other parameters and variables are same as the standard case.

CASE-IV: Both the volume flow rate and the electrophoretic mobility of bacteria are increased ten fold in this case. All the other parameters and variables have the same values as in the standard case.

CASE-V: In this case, the number of channels, n is fixed at 100 and the effect of varying length of the channel, L is observed. All the other parameters and variables have the same values as in the standard case.

CASE-VI: In the last case, the effect of varying the potential applied across the channel, V is observed. All the other parameters retain the original values as in the standard case.

As mentioned earlier, some direct bounds on the range of design variable values can be applied. For the current problem they are:

Lower bounds for n, W and H: 10, 1mm and 100 microns

Upper bounds for n, W and H: 600, 1m and 5mm.

Apart from the direct bounds on the range of design variables, additional constraints are imposed indirectly through other parameters. These constraints specify the relations between two or more design variables. For the current problem, they are:

$t_r < 900$ sec; $t_r/t_m > 3$;

$W/H > 25$; $W/H < 1000$;

4.5 RESULTS

The results of optimization for all the cases are compiled in the Table 4.2. On close inspection one can see that though there seems to be an optimal wetted volume for the device, there is no single set of channel dimensions for which minimum power is achieved. Also the number of channels keeps varying in each case. So we must judiciously pick a range of channel dimensions that are needed for our purpose and then select an appropriate number of channels to complete our device design.

TABLE 4.2: Optimization results for different test cases

	n	W	H	P/V	Vol	Power
CASE-1	80	4.66630E-01	9.64370E-04	3.98250E-05	1.80000E-03	7.16850E-08
CASE-2	390	9.57180E-01	9.64360E-04	3.98260E-05	1.80000E-02	7.16868E-07
CASE-3	90	1.31170E-01	3.04960E-03	3.98250E-06	1.80000E-03	7.16850E-09
CASE-4	120	1.00000E+00	3.00000E-03	4.11520E-06	1.80000E-02	7.40736E-08
CASE-5						
L=0.02	100	9.33130E-01	9.64240E-04	6.37710E-06	1.79950E-03	1.14756E-08
L=0.04	90	5.18480E-01	9.64370E-04	2.54880E-05	1.80000E-03	4.58784E-08
CASE-6						
V=0.3	130	5.24270E-01	5.28200E-04	1.32750E-04	1.80000E-03	2.38950E-07
V=0.5	80	6.59910E-01	6.81910E-04	7.96500E-05	1.80000E-03	1.43370E-07
V=0.75	80	5.38820E-01	8.35160E-04	5.31000E-05	1.80000E-03	9.55800E-08

We can see that as the length of the device increases, hydraulic power needed to sustain flow also increases. Also, hydraulic power needed decreases with increase in potential applied. This is because the channel separation can be increased since we have a higher potential available as the voltage applied increases. For the capture and concentration device, we can choose different wetted volumes and channel dimensions based upon the above discussion. Since fabricating is cheap for less number of channels and also since weight is directly related to the number of channels (more channels means more inlet and outlet connectors and more number of electrodes) it is better to have a range that approximately suits our requirements.

CHAPTER V

PHASE IV: COMPLIANCE WITH USER REQUIREMENTS

5.1   RESULTS AND DISCUSSION

This thesis is an effort to address the problem of volume mismatch between the day-to-day samples and the concentrated samples needed for analysis by the current state of the art bacterial detection systems. The main aim for this work is to come up with a conceptual design for the capture and concentration device, fabricate the device and demonstrate its performance. Extensive qualitative testing of the device is done and preliminary quantification results are presented.

5.2   ELECTROPHORETIC MOBILITY RESULTS

In Chapter III, the importance of electrophoretic mobility in design of the device was explained and the procedure for obtaining electrophoretic mobility of bacteria using capillary electrophoresis equipment was outlined. Electrophoretic mobility values of various bacteria grown in different starvation conditions and suspended in drinking water are presented in Table 5.1. Negative sign indicates that the bacterial cells are negatively charged and moving towards the anode. The electrophoretic mobility value for *E. coli* + GFP for minimal condition could not be determined since the *E. coli* culture has to be treated with antibiotics in the process of labeling it with GFP, and that killed the culture for minimal starvation state.

From Table 5.1, it can be seen that starved and dead cells, in general, have a higher mobility than viable cells. *Salmonella* in general has the least mobility values of

TABLE: 5.1: Electrophoretic mobility values for bacteria grown under different starvation conditions (Soni et. al., [55])

	Rich (cm^2/V-s)	Minimal (cm^2/V-s)	Starved (cm^2/V-s)	Dead (cm^2/V-s)
E.coli +GFP	-3.67x10^{-4} ±5.67x10^{-6}		-3.47 x10^{-4} ±1.98 x10^{-5}	-3.60 x10^{-4} ±9.32 x10^{-6}
Salmonella	-1.23 x10^{-4} ±1.17 x10^{-5}	-0.31 x10^{-4} ±3.25 x10^{-6}	-1.26 x10^{-4} ±1.88 x10^{-5}	-1.25 x10^{-4} ±1.88 x10^{-5}
*Pseudomon*as	-3.72 x10^{-4} ±4.32 x10^{-6}	-3.74 x10^{-4} ±2.44 x10^{-5}	-3.17 x10^{-4} ±1.36 x10^{-5}	-3.3 x10^{-4} ±2.11 x10^{-6}
E. coli	-3.81 x10^{-4} ±5.58 x10^{-6}	-3.13 x10^{-4} ±1.87 x10^{-6}	-3.23 x10^{-4} ±7.39 x10^{-6}	-3.37 x10^{-4} ±2.84 x10^{-6}

all the bacteria. *E. coli* and *Salmonella* cells grown in rich media have a higher mobility when compared to the same bacteria grown in minimal conditions, while there were no significant differences in the electrophoretic mobility of *Pseudomonas* cells when grown in rich or minimal medium. *Salmonella* grown in minimal media exhibits the least electrophoretic mobility value of all the bacteria. This value will be used in the design of the device since all the other bacteria move much faster and so the capture time for them will be smaller than that of *Salmonella* grown in minimal media.

5.3   PROOF OF CONCEPT

The original prototype (Figure 4.2) is used to demonstrate proof of concept about the principle of device. Experiments are conducted using carboxylate modified negatively charged 1.1 µm microspheres (Molecular Probes). A sample with a concentration of 2000
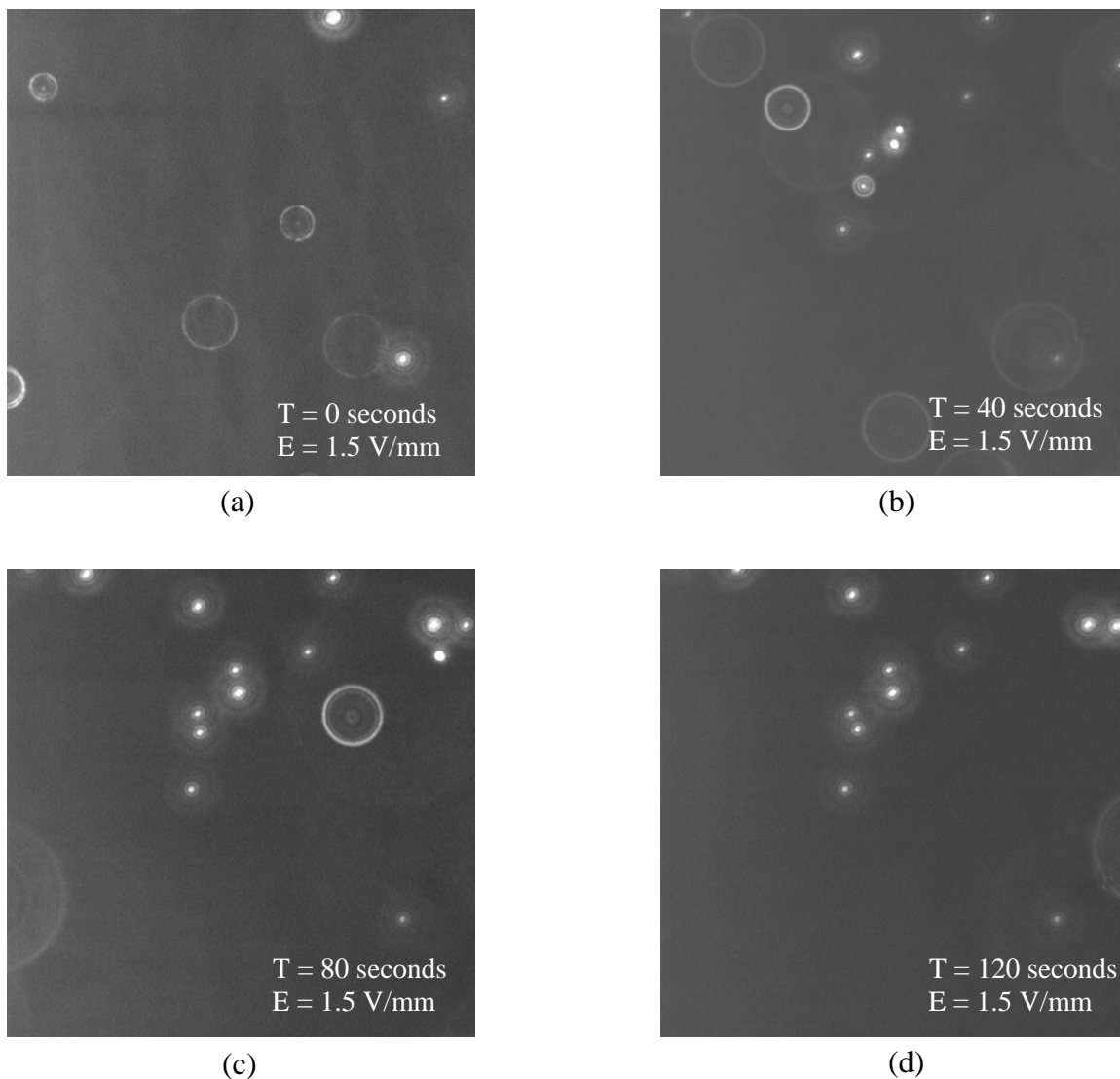
FIGURE 5.1: Capture of charged microspheres shown as a function of time. (a) Very few microspheres seen stuck to anode; (b) Many microspheres seen approaching the anode (Suggested by the out of focus particles); (c) Out of focus spheres are in sharper focus now; (d) All the spheres adhere to anode and are immobilized.

microspheres per ml is used. Since the volume of the channel is 0.7ml, a total of approximately 1400 microspheres are uniformly dispersed in the solution. All experiments were conducted without any flow in the channel.
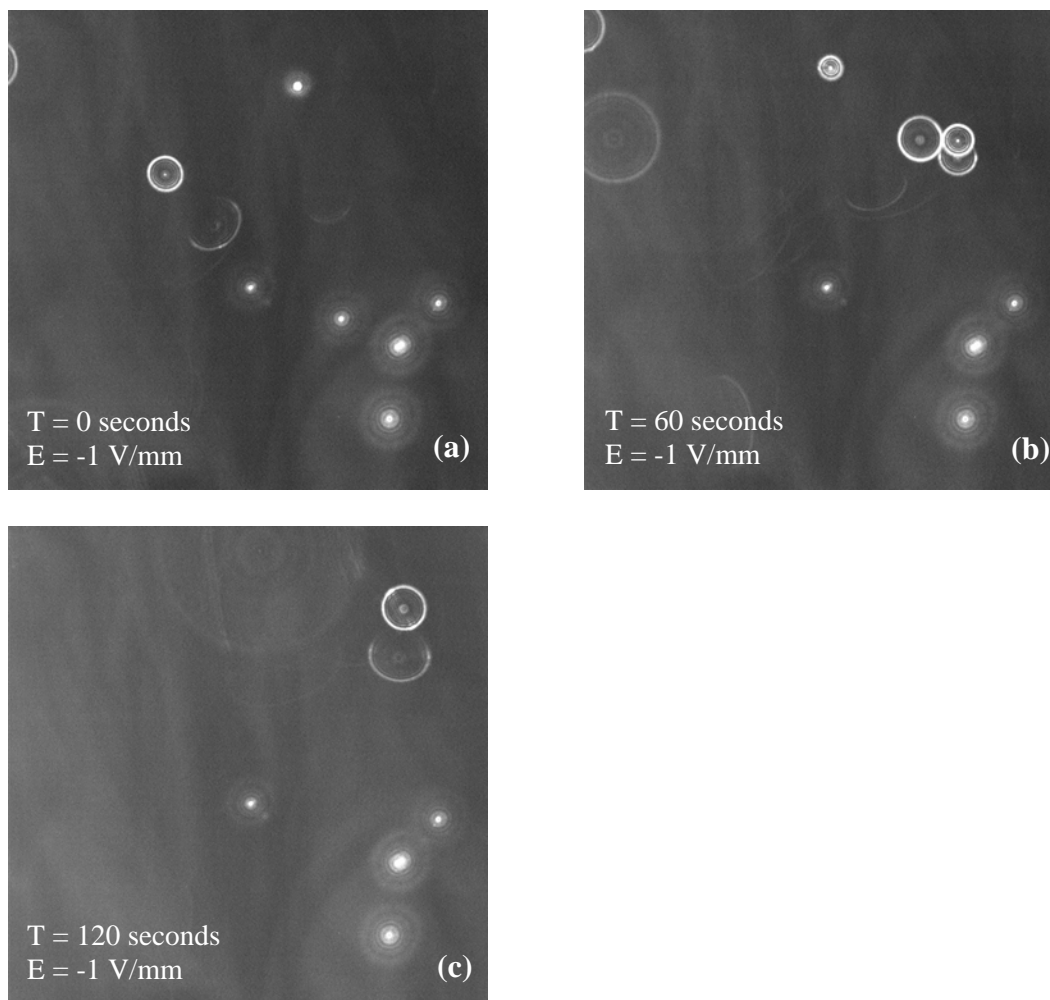
FIGURE 5.2: Release of charged microspheres shown as a function of time. (a) Electric field reversed and all spheres in focus; (b) Some spheres start to move out of focus plane; (c) Two spheres are released. Only partial release observed. High charge on microspheres causes irreversible adhesion.

Electrophoretic transport is observed under lateral electric field. Figure 5.1 shows

snapshots of the electrode surface taken at regular time intervals after application of the

electric field. Since the microspheres are tagged with fluorescent dye, they can be seen as

white dots attached to the electrode. Careful observation shows that there are some white dots with a halo around them (similar to diffraction patterns due to a small pin hole). They are actually out of focus microspheres that are either coming into the plane of focus or moving out of the view window. Capture is demonstrated by immobilized microspheres on electrode surface. Subsequently, the electric field applied to the electrodes is reversed in an attempt to reverse the adhesion of charged microspheres to the electrode. It is observed that most of the charged microspheres still remain attached to the electrode in spite of the adverse electric field acting on them. This behavior is attributed to the high charge on microspheres that leads to a strong irreversible adhesion onto the substrate. High shear due to flow, coupled with reversed electric fields is expected to release these particles. Figure 5.2 shows a time sequence of microsphere release on applying reversed electric fields.

5.4 QUALITATIVE STUDIES WITH *E. Coli*

The previous set of experiments, demonstrate our concept of electrophoretic transport and electrostatic trapping on the application of electric fields using charged dielectric spheres. Poortinga et al. [23] state that bacteria are also generally dealt with a theory (XDLVO theory) similar to one that governs dielectric charged surfaces (DLVO theory). As an extension to the previous set of experiments, capture and release of bacteria is also qualitatively studied using the old prototype. The same setup is used for experiments to show capture and release of *E. coli* grown in rich media. Figure 5.3 presents a time series of snapshots showing the capture of *E. coli*. The bacteria that are in focus and stuck to the electrode get immobilized and do not move, while those out of focus keep swimming and
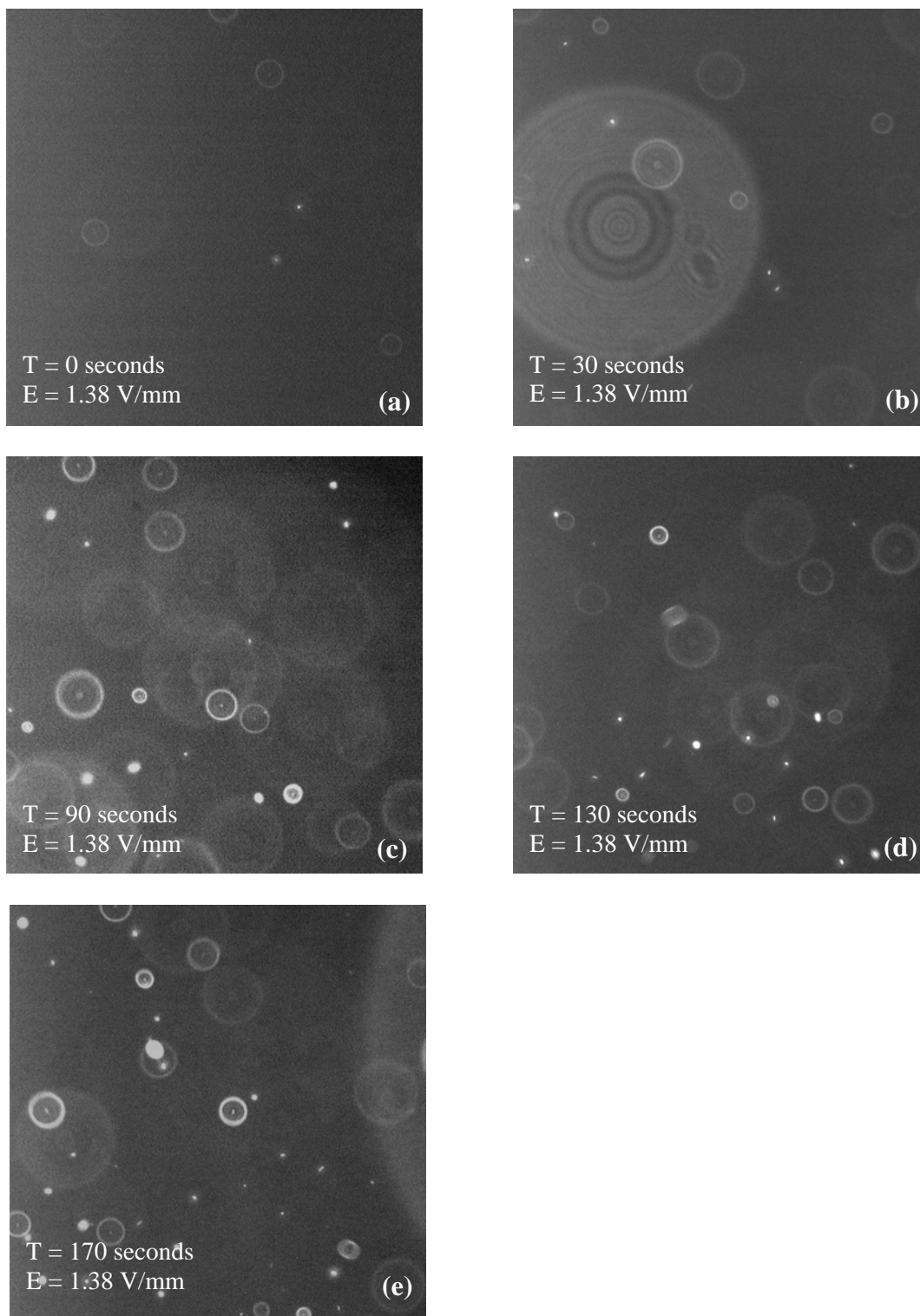
FIGURE 5.3: Capture of *E. coli* on anode shown as a function of time. (a) No bacteria on the anode surface; (b) Bacteria coming into plane of focus; (c) lots of bacteria out of focus but sizes shrinking, indicating that they are coming into focal plane; (d) Some bacteria seen to be attached to anode; (e) Many bacteria are in focus and immobilized.

eventually get stuck to the electrode either in the view window or at some other location on the anode, outside the view window.

Some bacteria, though under the influence of electric field, seem to be gliding over the electrode at a fixed separation. This form of adhesion, called mobile adhesion was also observed [56]. Mobile adhesion leads to bacterial aggregation over the electrode surface, since bacteria tend to form clusters rather than stay solitary. Figure 5.4 shows bacterial aggregation under electric field with time.

Release of *E. coli* under adverse electric fields was also qualitatively analyzed in an experiment similar to that performed with charged microspheres. Unlike microspheres, most of the bacterial adhesion is reversible as shown in Figure 5.5. According to these initial studies release of bacteria is possible just by reversing the electric fields. Applying shear will is expected to accelerate the process of release.

Even though capture and release of bacteria have been successfully demonstrated, there are other problems associated with the current prototype. Most prominent among them is the time scale for bacterial adhesion and release. The time for bacterial adhesion and release observed with the current device are inordinately high, defeating the very idea of developing a device for faster capture and concentration of bacteria. Also since the separation between the electrodes is large, even a high electric potential applied between the electrodes generates a weak electric field. The mobility time of bacteria can be reduced either by increasing the potential applied across the device or by reducing the separation between the electrodes.
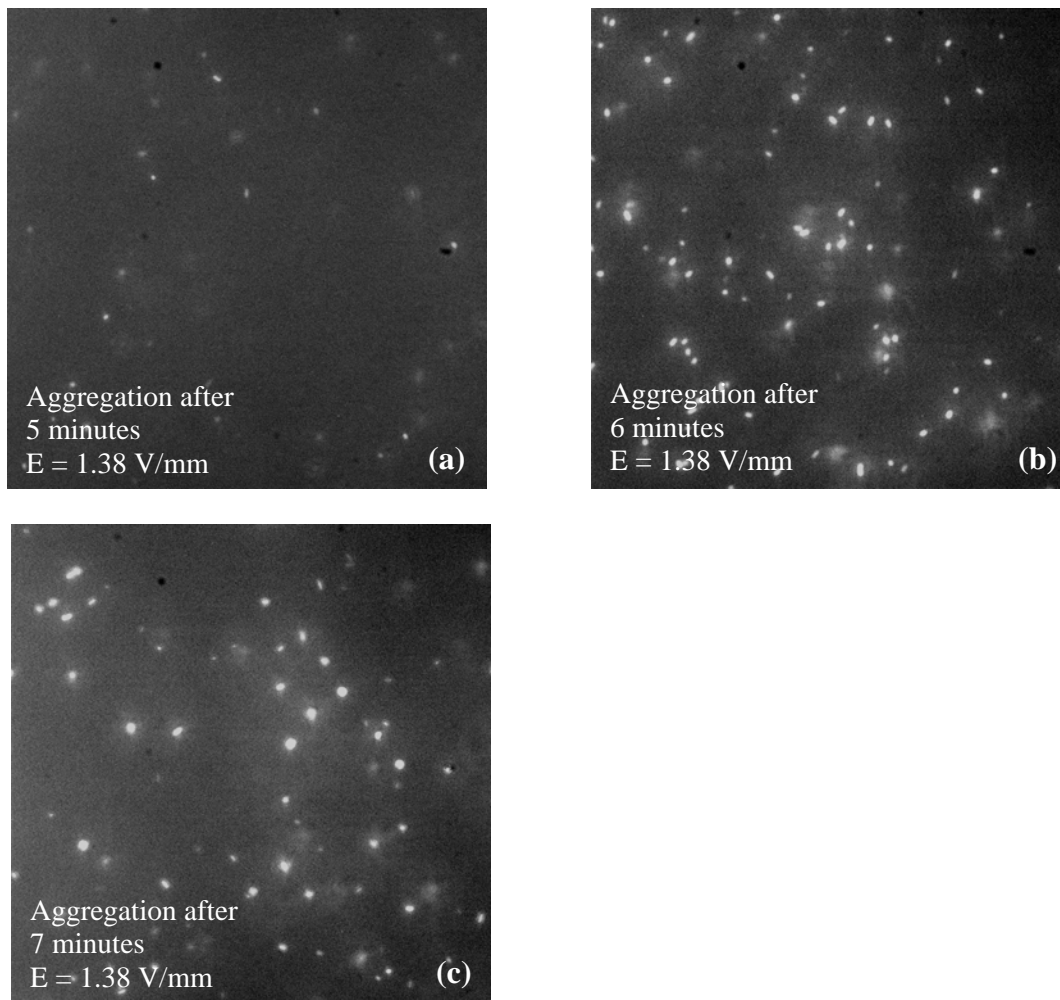
FIGURE 5.4: Aggregation of bacteria under the influence of electric field with time. (a) Only single bacteria can be seen and no clusters seen; (b) Smaller bacteria come together and aggregate to form clusters; (c) The cluster size increases further and very few single bacteria present.

Using the old prototype, a high voltage is needed to get an electric field that causes good electrophoresis of bacteria. But applying high voltage causes electrolysis of water (1.23V) and one sees bubble formation and pH gradients in the channel that are undesirable. Thus the electric field should be high at the same time the electric potential
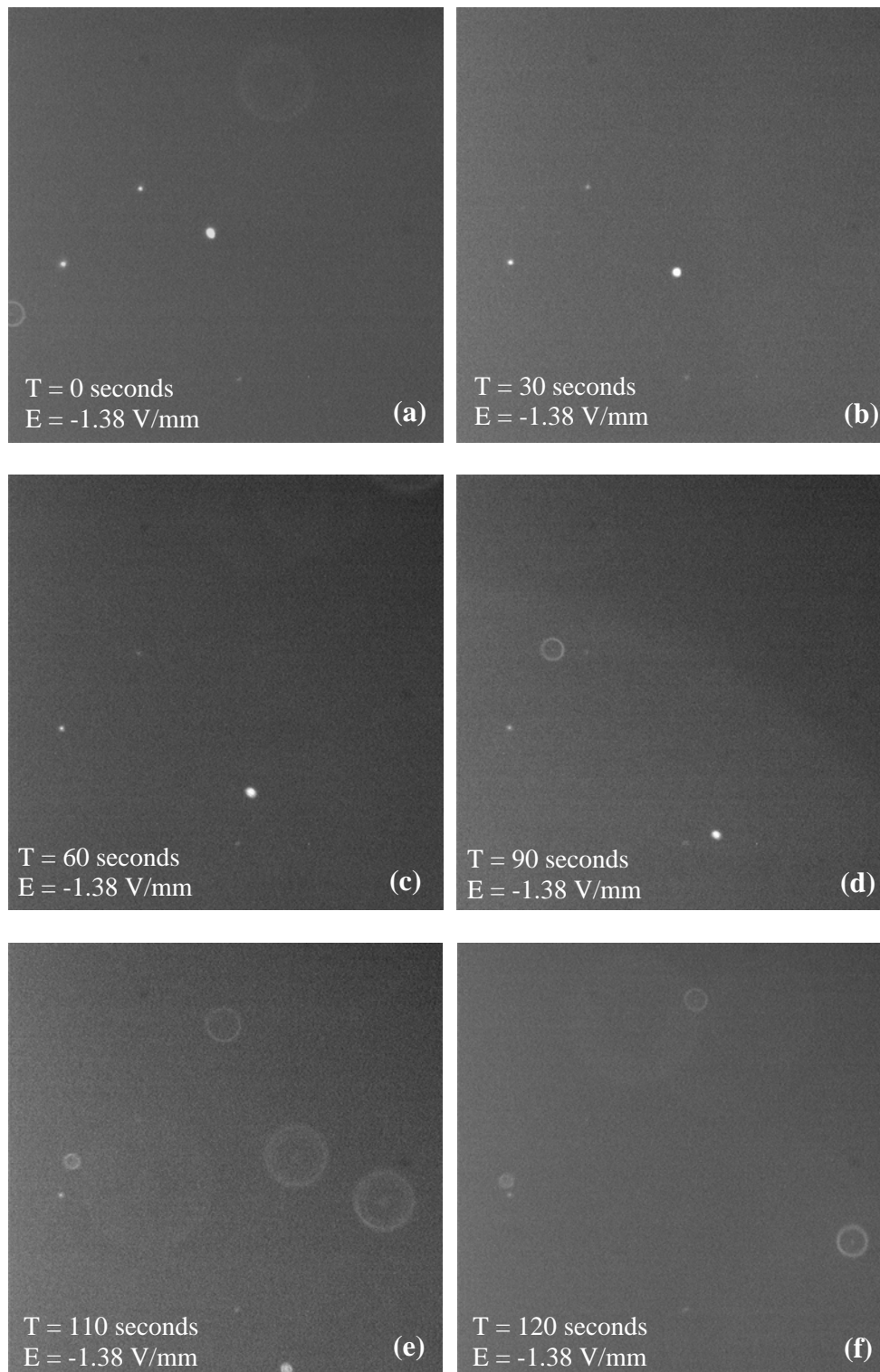
FIGURE 5.5: Release of *E. coli* under reversed electric fields as a function of time. (a) Electric field just reversed; (b), (c) & (d) One bacteria can be seen moving out of the plane; (e) & (f) All the bacteria get released and move out of the electrode plane.

has to be brought down below the electrolysis limit. Decreasing the separation between the electrodes will increase the electric field and also reduce the mobility time. So a new prototype is designed taking these factors into account, and the optimized channel dimensions are used in fabricating it. In the new device, electrodes will make up the sidewalls of channel as opposed to the previous device, where they formed the top and bottom walls of the channel. This enables observation of lateral motion of bacteria along the channel. In addition to qualitative studies, preliminary quantitative studies will also be conducted using this new prototype device. Design and fabrication of this device has been discussed in detail in Chapter IV.

5.5   INITIAL QUANTITATIVE RESULTS USING NEW PROTOTYPE

The proof of concept is illustrated using the new prototype in Figure 5.6. In the picture, electrodes are highlighted using red line. As seen, the top electrode is a cathode and the bottom one is an anode where all bacterial adhesion is observed. Also the bacteria can be seen to be clustering into colonies, rather than forming a uniform layer all over the anode. This type of bacterial clustering on application of electric fields has also been reported by Poortinga et al. [54].

Preliminary quantification results using DI water are shown in Table 5.2. Four-log reduction in bacteria concentration is observed at the outlet of the device when compared to the bacteria concentration at inlet. Results with drinking water have been omitted since

TABLE 5.2: Quantification of capture efficiency in DI water

Sample	Timeline min	Bacteria Concentration cfu/ml
Device filled with DI water	0	No sampling
DI water run for 10 min	0 - 10	No sampling
Collect DI sample for 15 min	10 - 25	10^2
E. coli flushing run – 15 min	25 - 40	No sampling
E. coli –ve control – 15 min	40 - 55	1.086×10^6 (6 log)
Electric field turned on	***Time Reset***	
E. coli sample – 15 min	0 - 15	6.0×10^2 (2 log)
E. coli sample – 15 min	15 - 30	10^3 (3 log)
E. coli sample – 15 min	30 - 45	6.85×10^3 (3 log)
E. coli sample – 15 min	45 - 60	2.6×10^4 (4 log)
Filter sterilized DI	N/A	Nil
Input *E. coli* sample	N/A	1.43×10^7 (7 log)

the analysis showed that there were no bacteria in the outlet sample. On close observation under microscope, we could still see many bacteria that were fluorescing green, indicating that they were still viable. This suggests that something in the device is making the bacteria unculturable when drinking water is used as the suspension media.

A closer observation of the electrode surface revealed that these bacteria were not only clustering among themselves, but also adhering to a gelatinous matrix type material that formed all over the electrode surface. Water analysis of these outlet samples showed a 700-fold increase in copper concentration, which is known to make bacteria unculturable. It was also observed that this matrix type material did not form with de-ionized water suggesting that there is some relation between the ionic content of water

and the formation of this matrix like substance. This hints to possible electrochemical reactions in the device leading to increased ionic content, and dissolution of copper into the electrolyte.
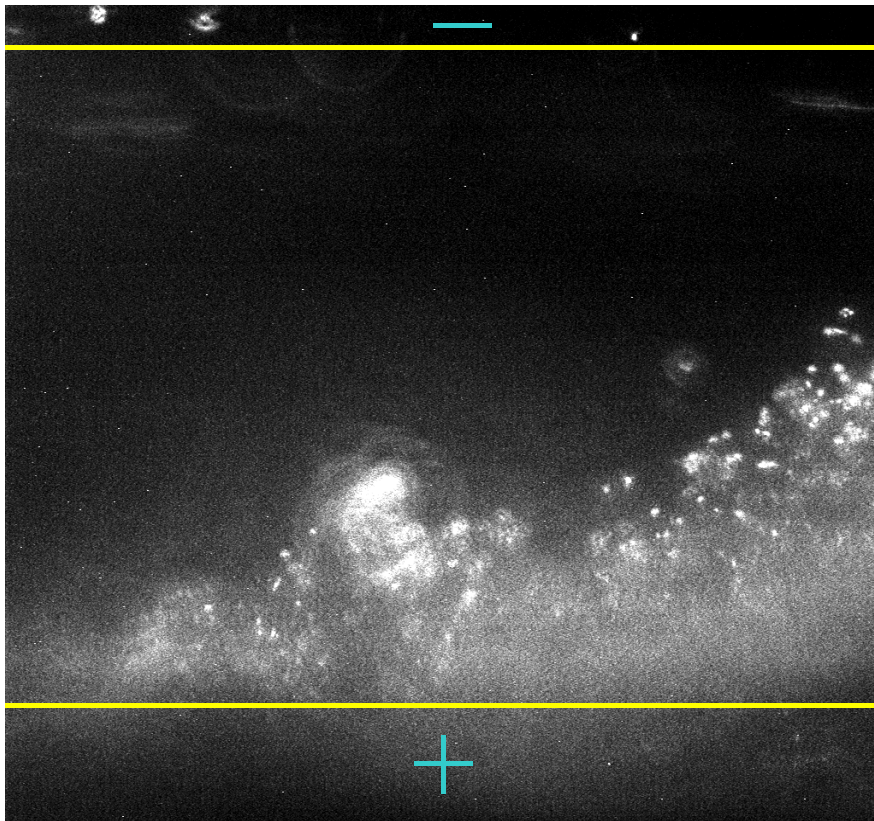
FIGURE 5.6: Figure showing formation of clusters on the anode.

CHAPTER VI

CONCLUSION AND FUTURE WORK

6.1 CONCLUSION

A microfluidic device for the capture and concentration of bacteria from drinking water was designed, fabricated and tested. The design involved three major phases:

1. Development of a prototype channel for demonstrating operation of the device

2. Incorporating the constraints into governing equations by optimizing the device for minimal power consumption and wetted volume and

3. Designing a new prototype for the purpose of qualitative studies and preliminary quantitative analysis.

The first prototype is developed to show proof of bacterial electrophoresis on the application of an electric field in a micro-channel. Flow is not used in this device, enabling qualitative studies of bacterial electrophoresis under the microscope. Problems related to low electric field strength, bubble formation due to application of high electric potential, pH gradients in the channel and large time scales for electrophoresis, affect the working of device. Since the device is fabricated for convenience of imaging and is not optimized for capture of bacteria, it cannot be used for quantification.

Once the concept is presented using a preliminary prototype device, optimization of the channel is performed. This ensures that all the design constraints are satisfied and we have the optimal values for the design variables. The optimized values are used in constructing a new prototype device that can address all the problems seen in the original

prototype. In solving these problems, some new observations related to electrochemistry and biocompatibility of electrode material were made. Using the new prototype, capture of bacteria under flow is demonstrated.

Both qualitative and quantitative studies are done using this device to study the effect of different design parameters on the capture of bacteria. Capture efficiency of the device is quantified. Using DI water as the suspension media, a 99.99% capture is observed. Encouraging observations from qualitative studies and preliminary quantitative results warrant further studies on using the principle of electrophoresis in a microfluidic channel for capture and concentration of bacteria.

6.2 FUTURE WORK

As mentioned earlier, there are some issues with the electrode material that have to be solved before a full-scale device is fabricated. The possibility of using an alternate metal for electrodes in place of copper, and electroplating gold instead of PVD to obtain an impervious gold layer are being studied. These changes should rectify most of the electrochemistry related problems, since the gold coating will be non-porous, eliminating the diffusion of substrate metal into electrolyte. Nickel has been found to be a good substitute for copper as a substrate metal for fabricating electrodes, but has been known to be toxic to humans. It also lacks the excellent machining qualities that copper has. Other alternatives like stainless steel etc. are being evaluated for substrate materials.

Alternately, a barrier layer of nickel or palladium can be used to prevent diffusion of copper through gold. Here, the electrodes will be machined using copper, and nickel or palladium will first be electroplated over the copper and this will be followed by gold. This is known to largely alleviate the problems of copper diffusion.

A multi channel device is also being designed to better quantify the capture efficiency of the process. The basic idea is to use commercially available electrodes and separate them using micro machined spacers or curable photoresists, by a gap of around 100 microns to result in a multi channel device. This will reduce the capture time to less than 5 minutes and increase the volumetric flow rate of water that is processed in the same amount of time. This essentially cuts down the running time for each experiment from 1 hour to around 15 minutes.

There are a couple of other minor problems that need to be addressed. First, changes should be made in the current design to make the new device leak proof. Marginal leaks were observed at high flow rates in the previous prototype. Next the inlet and outlet systems have to be designed in a way that they have a very low dead volume. In addition, the inlet mechanism should uniformly divide the flow between all the channels. Work is being done in this direction, and fabrication of a fully functional multi channel device is expected in the next couple of months.

REFERENCES

1. WHO/UNICEF, Global Water Supply and Sanitation Assessment 2000 Report, www.who.int, 2005.

2. R.C. Mroz and S.D. Pillai, Bacterial populations in the groundwater on the US-Mexico border in El Paso County, Texas. *Southern Medical Journal*, vol. 87, pp. 1214-1218, 1994.

3. T.M. Straub and D.P. Chandler, Towards a unified system for detecting waterborne pathogens, *Journal of Microbiological Methods*, vol. 53, pp. 185-197, 2003.

4. S.D. Pillai, Molecular methods for microbial detection, in *Pre-harvest and Post-harvest Food Safety: Contemporary Issues and Future Directions*, (eds. R.C.Bier, S.D. Pillai. T.D. Phillips, and R.L. Ziprin). Institute of Food Technologists/Iowa State Press, Ames, 2004 (in press).

5. D. Hoefel, W.L. Grooby, P.T. Monis, S. Andrews and C.P. Saint, Enumeration of water-borne diseases using viability assays and flow cytometry: A comparison to culture based techniques, *Journal of Microbiological Methods*, vol. 55, pp. 585-597, 2003.

6. M.C.M. Van Loosdrecht, J. Lyklema, W. Norde and A.J.B. Zehnder, Influence of interfaces on microbial activity, *Microbiological Reviews*, vol. 54, pp. 75-87, 1990.

7. M.S. Powell and N.K.H. Slater, The deposition of bacterial cells from laminar flows onto solid surfaces, *Biotechnology and Bioengineering*, vol. 25, pp. 891-900, 1983.

8. P.R. Rutter and T.V. Leech, The deposition of *Streptococcus-Sanguid NCTC-7868* from a flowing suspension, *Journal of General Microbiology*, vol. 120, pp. 301-307, 1980.

9. P.R. Rutter and A. Abbott, Study of interaction between oral *Streptococci* and hard surfaces, *Journal of General Microbiology*, vol. 105, pp. 219-226, 1978.

10. A. Aertsen and C.W. Michiels, Stress and how bacteria cope with death and survival, *Critical Reviews in Microbiology*, vol. 30, pp. 263-273, 2004.

11. D.B. Kell, A.S. Kaprelyants, D.H. Weichart, C.R. Harwood and M.R. Barer, Viability and activity in readily culturable bacteria: A review and discussion of the practical issues, *Antonie van Leeuwenhoek*, vol. 73, pp. 169–187, 1998.

12. M. du Preez, R. Kfir and P. Coubrough, Investigation of injury of coliforms after chlorination, *Water Science Technology*, vol. 31, pp. 115-118, 1998.

13. G.A. McFeters, M.W. LeChevallier, A. Singh and J.S. Kippin, Health significance and occurrence of injured bacteria in drinking water, *Water Science Technology*, vol. 18, pp. 227–231, 1986.

14. D.B. Kell and M. Young, Bacterial dormancy and culturability: The role of autocrine growth factors, *Current Opinion in Microbiology*, vol. 3, pp. 238-243, 2000.

15. P.W. Benoit and D.W. Donahue, Methods for rapid separation and concentration of bacteria in food that bypass time-consuming cultural enrichment, *Journal of Food Protection*, vol. 66, pp. 1935-1948, 2003.

16. S.M. Goyal and C.P. Gerba., Concentration of bacteria from large volumes of tap water, *Applied and Environmental Microbiology*, vol. 40, pp. 912-916, 1980.

17. B. Furrer, U. Candrian, C. Hoefelein and J. Luethy, Detection and identification cation of *Listeria* monocytogenes in cooked sausage products and in milk by *in vitro* amplification of haemolysin gene fragments, *Journal of Applied Microbiology*, vol. 70, pp. 372–379, 1991.

18. M.R. Blake and B.C. Weimer, Immunomagnetic detection of *Bacillus stearothermophilus* spores in food and environmental samples, *Applied and Environmental Microbiology*, vol. 63, pp. 1643-1646, 1997.

19. H.A. Pohl, *Dielectrophoresis*, Cambridge University Press, Cambridge, UK, 1978.

20. R.P. Burchard, D. Rittschof and J. Bonaventura, Adhesion and motility of gliding bacteria on substrata with different surface free energies, *Applied and Environmental Microbiology*, vol. 56, pp. 2529–2534, 1990.

21. Z. Liu and K.D. Papadopoulos, Unidirectional motility of *Escherichia coli* in restrictive capillaries, *Applied and Environmental Microbiology*, vol. 61, pp. 3567–3572, 1995.

22. M.A.S. Vigeant and Ford R.M., Interactions between motile *Escherichia coli* and glass in media with various ionic strengths as observed with a three-dimensional-

tracking microscope, *Applied and Environmental Microbiology*, vol. 63, pp. 3474–3479, 1997.

23. A.T. Poortinga, R. Bos and H.J. Busscher, Reversibility of bacterial adhesion at an electrode surface, *Langmuir*, vol. 17, pp. 2851-2856, 2001.

24. R.P. Feynman, There is plenty of room at the bottom, *Journal of Microelectromechanical Systems*, vol. 1, pp. 60-66, 1992.

25. K. Gabriel, J. Javris and W. Trimmer, Small machines, large opportunities, in *Micromechanics and MEMS: Classical and Seminal papers up to 1990*, pp. 117-143, IEEE Press, New York, 1997.

26. Grace R., Commercialization issues of MEMS/MST/Micromachines: An updated industry report card on the barriers to commercialization, *Sensors Expo Spring Proceedings*, San Jose, CA, 2002, 'available online at http://www.rgrace.com/Papers/papers.html'

27. G. E. Karniadakis and A. Beskok, *Micro Flows, Fundamentals and Simulations*, Springer Verlag, New York, 2001.

28. A. Beskok, J. Hahm and P. Dutta, Electrokinetic transport phenomena in micro-fluidics, in *Micromechanics and Nanoscale Effects: MEMS, Multi-Scale Materials and Micro-Flows*, pp. 81–116, Kluwer Academis Publishers, Boston, 2004

29. D.L. Jan, H. Lane and B. Wilson, Advanced Human Support Technology Program: Advanced Environmental Monitoring and Control Project Plan, NASA, http://taskbook.nasaprs.com/peer_review/prog/AEMC_Project.rtf, 1999.

30. K. Krishnakumar, "Material and Process Selection in Conceptual Design", Master's Thesis, Texas A&M University, College Station, TX, 2003.

31. T.R. Kulkarni and S.C. Suh, Crew Exploration Vehicle: Optimal design solutions and configuration, *American Institute of Aeronautics and Astronautics*, Albuquerque, NM, 2005.

32. F.F. Ruess, Sur un novel e_et de l'electricite galvanique, *Memoires de la Soci´et´e Imperiale de Naturalistes de Moskou,* vol. 2, pp. 327-336, 1809.

33. H.L.F. von Helmholtz, Studies of electric boundary layers, *Wied. Ann,* vol. 7, pp. 337-382, 1879.

34. P. Dutta and A. Beskok, Analytical solution of combined electroosmotic/pressure driven flows in two-dimensional straight channels: Finite Debye layer effects, *Analytical Chemistry,* vol. 73, pp. 1979-1986, 2000.

35. R.F. Probstein, *Physicochemical Hydrodynamics*, Wiley and Sons Inc., New York. 1994

36. G. Milazzo, *Electrochemistry: Theoretical Principles and Practical Applications*, Elsevier Publishing Company, New York, 1963

37. A.E. Herr, J.I. Molho, J.G. Santiago, M.G. Mungal, T.W. Kenny and M.G. Garguilo, Electroosmotic capillary flow with non-uniform zeta potential, *Analytical Chemistry*, vol. 72, pp. 1053-1057, 2000.

38. McClain M.A., Culbertson C.T., Jacobson S.C. and Ramsey J.M., Flow cytometry of *Escheria coli* on microfluidic devices, *Analytical Chemistry*, vol. 73, pp. 5334-5338, 2001.

39. R.B.M. Schasfoort, S. Schlautmann, J. Hendrikse and A.V.D. Berg, Field-effect flow control in microfabricated fluidic networks, *Science*, vol. 286, pp. 942-945, 1999.

40. C.R. Cabrera, B. Finlayson and P. Yager, Formation of natural pH gradients in a microfluidic device under flow conditions: Model and experimental validation, *Analytical Chemistry*, vol. 73, pp. 658-666, 2001.

41. K. Macounova, C.R. Cabrera and P. Yager, Concentration and separation of proteins in microfluidic channels on the basis of transverse IEF, *Analytical Chemistry*, vol. 73, pp. 1627-1633, 2001

42. Cummings E.B., Ideal electrokinesis and dielectrophoresis in arrays of insulating posts, *American Institute of Aeronautics and Astronautics*, (2001-1163), pp. 1-10, 2001.

43. Ermakov S.V., Jacobson S.C. and Ramsey J.M., Computer simulation of electrokinetic transport in micro fabricated channel structures, *Analytical Chemistry*, vol. 70, pp. 4494-4504, 1998.

44. R.J. Hunter, *Zeta Potential in Colloid Science: Principles and Applications*, Academic Press Inc., New York, 1981.

45. S.E. Dowd, S.D. Pillai, S.Wang and M.Y. Corapcioglu, Delineating the specific influence of virus isoelectric point and size on virus adsorption and transport through sandy soils, *Applied and Environmental Microbiology*, vol. 64, pp. 405-410, 1998.

46. D. Schulze-Makuch, H. Guan and S.D. Pillai, Effects of pH and geological medium on bacteriophages MS2 transport in a model aquifer, *Geomicrobiology Journal*, vol. 20, pp. 73-84, 2003.

47. A.E. Herr, J.C. Mikkelsen, J.G. Santiago, T.W. Kenny, D.A. Borkholder and M.A. Northrup, *Electroosmotic flow suppression and its implications for a miniaturized full-field detection approach to capillary isoelectric focusing*, 2000 ASME International Mechanical Engineering Congress and Exposition, Orlando, FL, 2000.

48. D. Belder, A. Deege, F. Kohler and M. Ludwig, Poly(vinyl alcohol)-coated microfluidic devices for high-performance microchip electrophoresis, *Electrophoresis*, vol. 23, pp. 3567-3573, 2002.

49. S.M. Ford, "Fabricating Microfluidic Devices in Polymers for Bioanalytical Applications", Master's Thesis, Louisiana State University, Baton Rouge, LA, 2001.

50. S.S. Rao, *Engineering Optimization – Theory and Practice*, Wiley Interscience Publication, New York, 1996

51. H.H. Bau, Optimization of conduits' shape in micro heat exchangers, *International Journal of Heat and Mass Transfer*, vol. 41, pp. 2717–2723, 1998.

52. X. Wei and Y. Joshi, Optimization study of stacked micro-channel heat sinks for micro-electronic cooling, *IEEE Transactions on Components and Packaging Technologies*, vol. 26, pp. 55-61, 2003.

53. *Matlab Optimization Toolbox*, Manual, Version 3.0.2, www.mathworks.com.

54. A.T. Poortinga, R. Bosand H.J. Busscher, Controlled electrophoretic deposition of bacteria to surfaces for the design of biofilms, *Biotechnology and Bioengineering*, vol. 67, pp. 117-120, 2005.

55. K.A. Soni, A.K. Balasubramanian, A. Beskok and S.D. Pillai, Delineating the Electrophoretic mobilities of environmentally stressed states of selected bacteria in drinking water, *Applied and Environmental Microbiology*, (2005), (submitted).

56. H.J. Busscher, A.T. Poortinga and R. Bos, Lateral and perpendicular interaction forces involved in mobile and immobile adhesion of microorganisms on model solid surfaces, *Current Microbiology*, vol. 37, pp. 319-323, 1998.

APPENDIX A

```
function [f,G] = objfungrad(x)
% Objective Function
%Q = 0.000001388888888;
Q = 0.000002;
eta = 0.001;
V = 1.0;
mu = 0.0000000031;
L = 0.05;
%Minimizing Power/Volume
% (12.Q^2.eta)/(n^2.w^2.h^4)
%Objective function
f = (12*(Q^2)*eta)/((x(1)^2)*(x(2)^2)*(x(3)^4));

%Gradient of the objective function
t = (12*(Q^2)*eta)/((x(1)^2)*(x(2)^2)*(x(3)^4));
G = [-2*t/x(1), -2*t/x(2), -4*t/x(3)];
%f = (12*x(1)*eta*Q^2)/(x(4)*x(2)*x(3)^3);
```

APPENDIX B

```matlab
function [c,ceq,DC,DCeq] = confungrad(x)
% Nonlinear Constraints
Q = 0.000002;
eta = 0.001;
V = 1.0;
mu = 0.0000000031;
L = 0.05;

% Nonlinear Inequality Constraints
%c = [2 - mu*V*x(4)*x(1)*x(2)/(x(3)*Q); mu*V*x(4)*x(1)*x(2)/(x(3)*Q) -
10; 5-x(2)/x(3); x(2)/x(3)-15];
%c = [3*(x(3))^2/(mu*V)-x(1)*x(2)*x(3)*x(4)/Q; 10*x(3)-x(2); 2*x(2)-
x(1); 1.1-x(4)];
%                tm<tr                          ;w/h>10        ;L/w>2

c = [x(1)*L*x(2)*x(3)/Q - 900;       %tr<900
    3*x(3)*Q - x(1)*x(2)*L*mu*V;     % tr/tm>3
    x(1)*x(2)*L*mu*V - 10*x(3)*Q;    % tr/tm<10
    25*x(3)-x(2);                    % w/h>25
    x(2)-1000*x(3)];                  % w/h<1000

% Derivatives of inequality constraints
DC = [L*x(2)*x(3)/Q, -x(2)*L*mu*V, x(2)*L*mu*V, 0, 0;       % d/dx(1)
     x(1)*L*x(3)/Q, -x(1)*L*mu*V, x(1)*L*mu*V, -1, 1;       % d/dx(2)
     x(1)*L*x(2)/Q, 3*Q, - 10*Q, 25, -1000];               % d/dx(3)


% Nonlinear Equality Constraints
%ceq = [];
ceq = [rem(x(1),1)];                            %n is an Integer


% Derivative of Equality constraints
DCeq = [1];
```

APPENDIX C

```
% In this program all the three design variables "n", "W", and "H" are
varied
!trip3=0;
for n=2:5:102
!    trip2=0;
 !   solution=[];
  !  for w=0.005:0.02475:0.5
         trip1=0;
     !    sol=[];
      !  for h=0.0005:0.000225:0.005
              %x0 = [2, 0.0130, 0.0006];    %Initial guesses
              x0 = [n, w , h];
              lb = [2, 0.005, 0.0005];    % Lower bounds
              ub = [600, 0.5, 0.005];    % Upper bounds
              options =
optimset('LargeScale','off','MaxFunEvals',10000,'MaxIter',1000);
              % Giving the function options
              [x,fval,exitflag,output] =
fmincon(@objfungrad,x0,[],[],[],[],lb,ub,@confungrad,options)
              %[x,fval,exitflag,output] = fminunc(@objfun,x0,options)
              [c,ceq] = confungrad(x)


              if trip1==0
                  trip1=1;
                  DV=x;
                  power=fval;
                  exf=exitflag;
              else
                  DV = [DV;x];
                  power=[power;fval];
                  exf = [exf;exitflag];
              end

         end

         sol=[exf, DV, power];
         if trip2==0
         trip2=1;
         solution=sol;
         else
         solution=[solution,sol];
         end

     end

     if trip3==0
     trip3=1;
     total=solution;
     else
     total=[total;solution];
     end

end

 dlmwrite('solution.xls',total,'\t');
```

VITA

Srinivas Cherla graduated with a B. Tech. degree in mechanical engineering from Jawaharlal Nehru Technological University, India in June 2002. He was ranked second in a graduating class of 62 students. He joined the Texas A&M University in the fall of 2002 for graduate studies in the mechanical engineering. He graduated with a Master of Science degree in mechanical engineering, in August 2005.

Srinivas Cherla may be contacted through Dr. Ali Beskok at the Mechanical Engineering Department, Texas A&M University, College Station, TX 77843-3123.